The Impact of Force Field on the Computational Screening of MOFs for CO_2 Separations

by

Derya Dokur

A Thesis Submitted to the
Graduate School of Sciences and Engineering
in Partial Fulfillment of the Requirements for
the Degree of

Master of Science
in
Chemical and Biological Engineering

Koç University
August 2019

Koç University

Graduate School of Sciences and Engineering

This is to certify that I have examined this copy of a master's thesis by

Derya Dokur

and have found that it is complete and satisfactory in all respects,
and that any and all revisions required by the final
examining committee have been made.

Committee Members:

_____

Prof. Seda Keskin Avcı (Advisor, Koç University)

_____

Assoc. Prof. Alper Uzun (Koç University)

_____

Asst. Prof. İlknur Eruçar Fındıkçı (Özyeğin University)

Date: _____

ABSTRACT

Metal-organic frameworks (MOFs) have been considered as highly promising materials for adsorption-based CO_2 separations. The number of synthesized MOFs has been increasing very rapidly. High-throughput molecular simulations are very useful to screen large numbers of MOFs in order to identify the most promising adsorbents prior to extensive experimental studies. Results of molecular simulations depend on the force field used to define the interactions between gas molecules and MOFs. Choosing the appropriate force field for MOFs is essential to make reliable predictions about the materials' performance. In this thesis, two sets of molecular simulations using the two widely used generic force fields, Dreiding and Universal Force Field (UFF), were performed and adsorption data of CO_2/H_2, CO_2/N_2, and CO_2/CH_4 mixtures in 100 different MOF structures were obtained. Using this adsorption data, several adsorbent evaluation metrics including selectivity, working capacity, sorbent selection parameter, and percent regenerability were computed for each MOF. MOFs were ranked based on these evaluation metrics, and top performing materials were identified. Then, the sensitivity of the MOF rankings to the force field type was examined. The results showed that although there are significant quantitative differences between some adsorbent evaluation metrics computed using different force fields, rankings of the top MOF adsorbents for CO_2 separations are generally similar: 8, 8, and 9 out of the top 10 most selective MOFs were found to be identical in the ranking for CO_2/H_2, CO_2/N_2, and CO_2/CH_4 separations using Dreiding and UFF. Finally, a force field factor depending on the energy parameters of atoms present in the MOFs was suggested to quantify the robustness of the simulation results to the force field selection. This easily computable factor will be highly useful to determine whether the results are sensitive to the force field type or not prior to performing computationally demanding molecular simulations. In the second part of this thesis, 4213 MOFs from Cambridge Structural Database were screened

using GCMC (Grand Canonical Monte Carlo) simulation to identify the most promising materials for H_2S separation from H_2S/CH_4 mixture. All performance metrics were computed for entire material database. Top performing MOFs were determined based on following strategy: The MOFs with high regenerability were ranked based on APS (adsorbent performance score) values for H_2S/CH_4 mixture. Top 20 performing materials were investigated using GCMC simulation for ternary mixture of $H_2S/CH_4/CO_2$ to obtain a more convenient evaluation for the industrial cases. The structure-performance relationship was elucidated to design a novel MOF exhibiting high H_2S separation potential. Results indicated that the MOFs with 3.8Å<PLD<5 Å, 5Å<LCD<7.5Å, $0.5<\phi<0.75$, 1 $g/cm^3<\rho<1.5 g/cm^3$ and SA<1000 m^2/g (1000 m^2/g<SA< 2000 m^2/g for top 20 in terms of APS) are the promising materials with respect to both selectivity and APS.

ÖZET

Bu tezde, metal-organik yapılar (MOF) kullanılarak yapılan ayırma işlemlerinde başvurulmak üzere MOF'ların performanslarına göre sıralanmasına etki eden parametreler incelenmiştir. Metal-organik yapılar, fiziksel ve kimyasal özellikleri sebebiyle, adsorpsiyona dayalı CO_2 ayırma işlemleri için oldukça gelecek vadeden malzemelerdir. Bugüne kadar binlerce MOF sentezlenmiş olup, sentezlenen MOF sayısı her geçen gün artmaktadır. Kapsamlı deneysel çalışmalar yapılmadan önce performansı en iyi olan adsorbentlerin belirlenmesinde, yüksek verimli moleküler simülasyonlar çok sayıda MOF'un taranmasını büyük ölçüde kolaylaştırmaktadır. Moleküler simülasyonlardan elde edilen sonuçlar, gaz molekülleri ile MOF'lar arasındaki etkileşimlerin tanımlanması için kullanılan kuvvet alanına bağlı olarak değişmektedir. Malzemelerin performansı ile ilgili güvenilir tahminler yapılabilmesi için MOF'lara uygun kuvvet alanının seçilmesi gerekmektedir. Bu tez çalışmasında, yaygın şekilde kullanılan iki jenerik kuvvet alanı olan Dreiding ve UFF kullanılarak iki grup moleküler simülasyon yapılmış ve CO_2/H_2, CO_2/N_2 ve CO_2/CH_4 karışımlarının 100 farklı MOF yapısı içindeki adsorpsiyon verileri elde edilmiştir. Bu adsorpsiyon verileri kullanılarak, seçicilik, çalışma kapasitesi, sorbent seçim parametresi ve yenilenebilirlik yüzdesi dahil olmak üzere çeşitli adsorbent değerlendirme kriterleri her bir MOF için hesaplanmıştır. Daha sonra, MOF'lar bu değerlendirme kriterlerine göre sıralanarak, en iyi performansı gösteren malzemeler belirlenmiş ve MOF sıralamasının kuvvet alanı türüne olan hassasiyeti incelenmiştir. Elde edilen sonuçlar, farklı kuvvet alanları kullanılarak hesaplanan bazı adsorbent değerlendirme kriterleri arasında anlamlı kantitatif farklılıklar olmasına rağmen, CO_2 ayırma işlemleri için en iyi performans gösteren MOF adsorbentleri sıralamasının genel olarak benzer olduğunu ortaya koymuştur: en seçici ilk 10 MOF'un 8, 8 ve 9'unun Dreiding ve UFF kullanılan CO_2/H_2, CO_2/N_2 ve CO_2/CH_4 ayırmalarında sıralama açısından aynı olduğu bulunmuştur. Son olarak, simülasyon sonuçlarının kuvvet alanı

seçimine olan duyarlılığının kantitatif olarak belirlenmesi amacıyla MOF'larda bulunan atomların enerji parametrelerine bağlı bir kuvvet alanı faktörü tanımlanmıştır. Kolaylıkla hesaplanabilen bu faktör, kapsamlı hesaplamalar gerektiren moleküler simülasyonlar yapılmadan önce, sonuçların kuvvet alanı türüne karşı hassas olup olmadığının belirlenmesini oldukça kolaylaştıracaktır. Bu tezin ikinci kısmında, Cambridge yapı veri tabanından alınan 4213 MOF, H_2S/CH_4 karışımından H_2S'in ayrılmasında kullanılmak üzere en çok gelecek vadeden malzemelerin belirlenmesi amacıyla GCMC simülasyonu kullanılarak taranmıştır. Tüm performans kriterleri, malzeme veri tabanının tamamı için hesaplanmıştır. En iyi performans gösteren MOF'lar şu stratejiye göre belirlenmiştir: yenilenebilirliği yüksek olan MOF'lar, H_2S/CH_4 karışımına yönelik APS değerlerine göre sıralanmıştır. En iyi performans gösteren ilk 20 MOF, gerçek endüstriyel uygulamalar açısından daha elverişli bir değerlendirme sağlanması amacıyla $H_2S/CH_4/CO_2$ üçlü karışımı için GCMC simülasyonu kullanılarak incelenmiştir. H_2S ayırma açısından yüksek potansiyel sergileyen yeni bir MOF tasarlamak için yapı-performans ilişkisi aydınlatılmıştır. Elde edilen sonuçlar, $3.8Å<PLD<5$ Å, $5Å<LCD<7.5Å$, $0.5<\phi<0.75$, $1\ g/cm^3<\rho<1.5g/cm^3$ ve $SA<1000\ m^2/g$ (APS açısından ilk 20 malzeme için $1000\ m^2/g<SA<2000\ m^2/g$) değerlerine sahip olan MOF'ların, hem seçicilik hem de APS bakımından gelecek vadeden malzemeler olduğunu göstermiştir.

ACKNOWLEDGEMENTS

I, first of all, would like to thank Prof. Seda Keskin for not only being my advisor, but also for her deep understanding and great patience from the very beginning of my graduate study period that was full of challenges. She has tirelessly and kindly supported me in every case I need, which I do appreciate a lot. I will definitely keep the learnings from her in my mind and benefit from the experiences with her for the rest of my life.

I would also like to thank Assoc. Prof. Alper Uzun for his valuable lecturing during my graduation program and accepting to be in my thesis committee. I also need to thank Asst. Prof. İlknur Eruçar Fındıkçı for her important support to our works in NEMO group and accepting to be in my thesis committee.

I should especially thank Çiğdem for her worthwhile support throughout my graduation period. I will always remember her as a patient and helpful fellow. I also need to thank NEMO group members: Zeynep, Pelin, Burak, Vahid, Özge, Ayda, Gökay, Muhammed, Hilal, Mert, Harun, Safiyye, Sadiye, Gökhan, for their lovely friendships.

I would also like to thank my company, TÜPRAŞ, for the valuable convenience they provided me all the time via the Production Group Manager, Emre Kuzu, the Production Manager, Ahmet Cemil Karaoğuz, and the Operations Superintendent, Serhat Armutçu.

Lastly, I should thank my husband Eray, and my elder sister, Deniz, for their endless moral supports, and I deeply thank my beloved mother, Hüsniye, to whom I dedicated this thesis.

Also, the financial support provided by European Research Council (ERC) under the European Union's Horizon 2020 research and innovation programme (ERC-2017-Starting Grant, grant agreement No 756489-COSMOS) is gratefully acknowledged.

Derya Dokur

1 August 2019

TABLE OF CONTENTS

LIST OF TABLES

LIST OF FIGURES

NOMENCLATURE

acc	:	Acceptance criteria
AMBER	:	Assisted model building with energy refinement
APS	:	Adsorbent performance score
C_2H_5OH	:	Ethanol
CCDC	:	Cambridge Crystallographic Data Centre
CH_4	:	Methane
CO_2	:	Carbon dioxide
DFT	:	Density Functional Theory
SAPT	:	Symmetry-adapted perturbation theory
EQ_{eq}	:	Extended charge equilibration method
FF	:	Force field
FFF	:	Force field factor
GCMC	:	Grand Canonical Monte Carlo
h	:	Planck constant
H_2	:	Hydrogen
k_B	:	Boltzmann constant
LCD	:	Largest cavity diameter
LPD	:	Limiting pore diameter
μ	:	Chemical potential
m	:	Mass of gas atom
MC	:	Monte Carlo
MM	:	Molecular mechanics
MOF	:	Metal organic framework
MP2	:	Møller–Plesset second-order perturbation theory
N	:	Uptake

N_2	:	Nitrogen
NH_3	:	Ammonia
OPLS	:	Optimized potentials for liquid simulations
q	:	Partial atomic charge
QM	:	Quantum mechanics
PBE	:	Perdew-Burke-Ernzerhof
R%	:	Regenerability
R^2	:	Correlation coefficient
S	:	Selectivity
s	:	Fractional Coordinates
SRCC	:	Spearman's ranking correlation coefficient
T	:	Temperature
U	:	Molecular energy
UFF	:	Universal force field
V	:	Volume
β	:	Thermodynamic temperature
ΔN	:	Working capacity
ε	:	Potential well depth
Λ	:	Broglie wavelength
σ	:	Potential diameter
Ω	:	Partition function

Chapter 1

Introduction

With the rapid increasing demand in the fossil fuels as a result of population growth and industrialization, CO_2 capture and separation have become more and more important in recent decades. CO_2 level in the atmosphere is rising by burning of fossil fuels and high CO_2 concentration creates disturbance on carbon balance and causes global warming. Thus, it is crucial to mitigate the release of CO_2 to the atmosphere.[1] On the other hand, alternative hydrocarbon sources to petroleum, such as natural gas from landfill or shale gas and refinery fuel gas, are valuable due to their potentials of providing energy source. CO_2 separation from natural gas (CO_2/CH_4), power plant flue gas (CO_2/N_2) and petroleum refineries (CO_2/H_2) aims to decrease CO_2 emission. There are several methods to separate CO_2 from gas mixtures, such as absorption, cryogenic distillation, membrane separation, and adsorption, but low cost and energy requirement with acceptable operating conditions are essential.

Absorption is based on chemical or physical process which occurs between gas mixture and CO_2 selective absorbent. Although highly CO_2 selective absorbent provides low CO_2 concentration in treated gas mixture, further use of absorbent is costly due to more energy requirement of regenerability. Most absorbents have a trade-off between selectivity and regenerability, and it can be overcome by using different absorbents together.[2]

CO_2 is separated from gas mixtures based on phase change of CO_2 in cryogenic distillation. Phase change is provided by compressing and cooling of mixture with several stages. Liquid or solid CO_2 is formed as a result of this process depending on the

operating conditions and existence of water in mixture. Cryogenic distillation is an advantageous separation method in terms of high CO_2 recovery and easy transportation of CO_2 however, it is not suitable for mixtures with low CO_2 concentration and very costly due to the nature of process.[3]

Adsorption utilizes the intermolecular forces between gas molecules and solid surface of adsorbents. Gas molecules reversibly adhere to the surface of adsorbent in proportion to selectivity of gas. Efficiency of adsorption is affected by operating temperature and partial pressure of CO_2, pore size and available surface area of adsorbent and intermolecular forces between adsorbent and gas molecules. Adsorption process is a cost effective technology.[2] Thus, it is very important to identify the most effective adsorbents for CO_2 separation. Since some adsorbents suffer from low selectivity and working capacity, choosing of the proper adsorbent is crucial.

Various adsorbents have been already used for CO_2 separation, such as zeolites and activated carbon.[4] Metal-organic frameworks (MOFs) have strong potential to become alternatives to these traditional adsorbents for CO_2 capture.[5] MOFs have attractive physical and structural properties, such as low density (0.2-1 g/cm^3), high surface areas (500-4500 m_2/g), high porosities and reasonable thermal and mechanical stabilities.[6-9] Several studies investigated adsorption-based CO_2 separation performances of MOFs.[10-13] A comparison of different porous adsorbents, including MOFs, zeolites and activated carbons, shows that MOFs can outperform zeolites and carbon-based adsorbents due to their high CO_2 selectivities and working capacities.[14]

MOFs are composed of organic linkers connected by metal cation. During synthesis or design, physical and chemical properties can be adjusted by the combination of various metal complexes and organic ligands. This flexible synthesis procedure provides a large number of MOFs with a large versatility in geometry, pore size, and chemical functionality.[15] Besides the availability of many different materials is an advantage, it is also a significant challenge to find the optimal MOF among thousands for a specific

application. Although thousands of MOFs have been synthesized to date, limited fraction of these materials has been tested using purely experimental techniques. On the other hand, testing thousands of MOFs at the lab-scale is simply impractical. Therefore, molecular simulations have been successful to provide atomistic insights into gas adsorption in MOFs. The most important contribution of molecular simulations is to screen a large number of MOFs in a time-effective manner to identify the most promising materials for desired applications in order to guide the experimental efforts, time and resources to these promising materials.[16-19]

Molecular simulation of MOFs for gas adsorption is performed by using Grand Canonical Monte Carlo (GCMC)[20] techniques which is explained in detailed Chapter 3. The main and perhaps the most important input of the molecular simulation is the physical and chemical interactions between porous material and gas molecules. These interactions are described by a set of equations and parameters, known as force fields (FFs). Thus, the choice of the FFs directly affects the results of simulation. Successful application of molecular simulation requires accurate FFs for making reliable predictions about materials' performances.

At the early stages of the molecular simulation studies of MOFs, efforts have been made to develop the new FFs specific to MOF-gas interactions using quantum-level calculations.[21-22] These calculations are computationally demanding and troublesome for implementation to large number of materials. Thus, they can be performed for a very small number of MOFs but not for screening large number of materials. Tafipolsky and co-workers used the experimental, structural, and spectroscopic data in combination with quantum-level calculations to derive the FFs.[23] They confirmed experimental crystal structure of MOF-5 and vibrational infrared spectrum with this FF.

Moreover, there are other works which refined the generic FF parameters to better match the predictions of molecular simulations with the available experimental measurements of gas adsorption in MOFs.[22, 24-27] However, experimental data is only

available for very small number of materials among thousands of available MOFs. Many MOFs are lacking the experimentally measured gas adsorption isotherms to validate the FF.

Since developing a new generic or system-specific FF is very challenging and computationally demanding, ready to be used generic force fields are utilized for molecular simulation studies. Two off-the-shelf, generic FFs, Dreiding[28] and UFF[29], are very commonly used in molecular simulations of MOFs. Several studies used UFF or Dreiding force field in molecular simulation and compared the results of simulation data with experimentally measured uptake data.[16, 30] They reported generally good agreement between simulation and experiment and validated the usage of generic force fields for MOFs.

In another study, molecular simulation was performed for CO_2 and CH_4 adsorption of 424 hypothetical MOFs using both the UFF and ab initio FF.[31] Results presented that gas uptakes predicted by the generic FF and ab inito FF are quite different. Despite these quantitative differences in gas uptake, they obtained good correlation between the relative rankings of MOFs in terms of absolute gas uptake capacities predicted by different FFs. It was concluded that it may be a reasonable approximation to employ UFF in identifying the top percentage of MOFs for a particular gas adsorption application, but caution is still warranted. This thesis focused on the single-component gas uptake. However, FF type can affect more the result of gas mixture adsorption than the one of the single-component gas uptake because of competitive and/or collaborative effects between different gas species of a mixture for the same adsorption sites of the MOFs.

Due to these reasons, FF selection in the molecular simulation of MOFs is a very critical step to identify the promising materials for a particular purpose among thousands. Motivated from this issue, the impact of FF type on molecular simulation results was investigated in this thesis.

In this thesis, it was aimed to clarify how the different FFs make change in molecular simulation results. Molecular simulations were performed to compare the results from two different generic FFs, Dreiding and UFF, by computing adsorption of CO_2/H_2, CO_2/N_2 and CO_2/CH_4 mixtures in 100 different MOF structures. Using the gas adsorption data, four adsorbent evaluation metrics, adsorption selectivity, working capacity, sorbent selection parameter, per cent regenerability were computed for each MOF and for each gas separation. The metrics obtained from molecular simulations using different FFs were first compared to understand their sensitivities to the FF type. MOFs were then ranked based on these performance evaluation metrics to identify the top 10 best materials for separation of CO_2/H_2, CO_2/N_2 and CO_2/CH_4 mixtures. The MOFs that appear in the highly promising materials list of Dreiding and UFF-based molecular simulations were compared and robustness of the material rankings with respect to the FF type was discussed. Chapter 2 introduced the literature review on the development and application of different FFs. Limitations and differences of the force fields were displayed for molecular simulation studies conducted, particularly with MOFs. Details of computational methodology and theorical background were explained in Chapter 3. In Chapter 4, results of the molecular simulations for CO_2/H_2, CO_2/N_2 and CO_2/CH_4 mixtures were presented. Separation performances of MOFs were compared and the robustness of the materials ranking with respect to the FF type was discussed. A factor which depends on the structural properties of MOFs was proposed in order to understand the sensitivity of MOF to FF type for simulators. Finally, the findings were summarized and concluding remarks were given in Chapter 5.

Chapter 2

Literature Review

Molecular simulation of MOFs for adsorption should involve the intermolecular interactions between adsorbate and adsorbent in addition to the intramolecular interactions of adsorbate and adsorbent themselves. These interactions include non-bonded and bonded interactions that are described by the force fields. Bonded energy is in relation to the covalently bonded atom. It is sum of the bond stretching, bond angle and torsional angle. Besides, Van der Waals (vdW) and electrostatic interactions are components of the non-bonded energy.[32] Van der Waals energy consists of the short-range repulsive exchange potential and the attraction due to London dispersion. Electrostatic interaction is the result of the atomic partial charge of adsorbent atoms and the polarity of adsorbate.[33-34]

In the literature, there are two methodologies to model the energy of the system: quantum mechanics (QM) and molecular mechanics (MM). Quantum mechanics (first-principle or ab initio method) is based on the electronic structure calculation with Schrödinger equation or its analogs, and wave function or electron distribution is used to determine the all parameters.[34] Molecular mechanics (Westheimer method or force field method) utilizes the classical mechanics model for the equation of motion rather than electron-based calculation. This empirical method is used to apply the experimental data of the small molecules to large systems based on the classical mechanics approach.[34-35]

Various generic force fields were developed to predict the molecular structure and energy for the application in the field of molecular mechanics. Beginning of the development of force fields can be based on the spring-mass model defined by Andrews.[36]

MM1, MM2, MM3, and MM4 are the examples of derived force field by Allinger and co-workers.[35, 37-39] AMBER (Assisted model building with energy refinement)[40] was developed firstly for nucleotides and proteins, and then applied to the other materials including MOFs. OPLS (Optimized potentials for liquid simulations)[41] force field was derived for the crystals of cyclic peptides and crambin using bonded interactions from AMBER but Jorgensen and Julian Tirado-Rives developed non-bonded interactions. Further, Jorgensen et al.[42] improved and tested the first version of OPLS for organic liquids, and the new version is more widely used. Williams focused on the non-bonded interactions for crystalline aromatic hydrocarbons and crystalline hydrocarbons.[43-44] He used the interplanar spacing and compressibility of graphite to calculate C-C repulsion term in Van der Waals interactions. His work was a pioneer to derive the Dreiding force field. Dreiding[28] is based on general force constant and geometry parameters instead of individual force constant and atom-pair specific geometry parameters. UFF[29] is another force field that is widely used in molecular simulations. It utilizes hybridization and connectivity of element and serves for the entire periodic table. Addicoat et al.[45] tuned UFF parameters to ensure reliability of structure and extended parameters to use for transition metals. This force field, UFF4MOF, is specifically customized for MOFs.

These generic force fields are derived using same or different but mostly similar semi-empirical function to predict both bonded and non-bonded interactions. For example, AMBER uses 12-6 Lennard-Jones potential, whereas MM2 and MM3 force fields use the Exp-6 form for non-bonded vdW interactions.[46] Each terms used in Dreiding and UFF were explained in detail in Chapter 3.

In quantum method, the total energy of the system is determined from electron-based calculation and then force field parametrization is executed by fitting the calculated energy to classical mechanics function. The procedure of first-principle force field derivation is: 1) QM method selection and calculation of energy for different

configurations; 2) fitting the energy to the selected semi-empirical function; and 3) validation of the results with experimental data.[47]

Most studies developed first-principle force field and then applied it to the molecular simulation of MOFs for adsorption. They used different QM method or the combination of QM/MM, such as MP2, DFT-SAPT, DFT, PBE or NEMO method, and potential form, such as Lennard-Jones 12-6, Buckingham exponential-6, Morse potential, modified Buckingham potential, or the combination of them with or without electrostatic potential.[23, 47-49] While some works took both bonded and non-bonded interactions into account for the basis of calculation,[50-53] some of them included only non-bonded interactions in calculations.[54-57]

First-principle FFs are more accurate than generic ones. Molecular simulation of MOFs for adsorption of CO_2,[56, 58] CH_4,[59] H_2,[57] NH_3,[60] and C_1-C_4 alcohols[61] exhibits a very good agreement with experiment in terms of gas uptake. Numeric values of uptakes from ab initio calculations are significantly close to the experimental ones, whereas generic force fields slightly deviate from experimental data. Especially, generic FFs may not be capable of taking the interaction between adsorbate and open metal site in MOFs into account. For example, Dzubak et al. developed a first-principle force field using MP2 method with NEMO decomposition and then fitted the energy to modified Buckingham potential in order to obtain ready parameters for CO_2 capture.[58] On the other hand, some studies included only the interaction between open metal and adsorbate in the quantum level calculations but other interactions are defined by generic force field, such as UFF[62-65] or OPLS.[66] Further, generic force fields do not provide accurate results for flexible MOFs. While bonded interactions are determined with quantum level calculations (DFT), non-bonded interactions are defined conventionally for flexible MOFs.[67-69]

Even though quantum level calculation is highly in agreement with experiment, it is not feasible to apply these calculations to the molecular simulation of MOFs. Quantum mechanics calculation can only be performed to a very small system since extraordinary

computational cost is required.[70] It is obvious that first-principle FFs are a certainly time-consuming and effort-demanding way to include Van der Waals interaction in the simulation in contrast to generic ones.

However, generic FFs are more convenient to examine the large systems or to perform large screening of MOFs due to their transferability. Gas adsorption prediction with generic FF can moderately be different from experimental data but it provides quick and useful insight to determine the promising materials. Therefore, the results from studies using generic force field provide satisfactory data as the starting point.

Numerous molecular simulation studies apply the generic FFs to compute the gas adsorption in MOFs for various purposes, such as CO_2 capture. Some studies use Dreiding force field for CO_2 capture in 20[71] and 14[72] different MOFs to explore the effect of electrostatic interactions. Their results are consistent with the experiments. Babarao and co-workers[73] utilized UFF for the interactions between CO_2 and CH_4 molecules, and IRMOF-1. They compared adsorbents of C_{168}, silicate and IRMOF-1 in terms of performance metrics. They also performed the first study to characterize extra-framework and reported extraordinary CO_2 selectivity for CO_2/CH_4, CO_2/H_2, and CO_2/N_2 mixtures in rho-ZMOF.[74]

Generic force fields are used to describe the interaction between adsorbate and adsorbent, especially for the large screening of MOFs for adsorption in molecular simulation studies. Colón and colleagues[75] created 18383 porous crystalline structures using crystal enumeration algorithms and investigated their structure-performance relationship for H_2 storage. They used UFF in molecular simulation to define adsorbent-adsorbate interaction. Wilmer et al.[76] performed a similar molecular simulation study using UFF with 137953 hypothetically generated MOFs for CH_4 storage. Qiao et al.[77] conducted an analysis on 4764 MOFs for CO_2 capture from flue gas and natural gas to find the properties of the most promising materials. In addition to adsorption studies, Watanabe and Sholl[78] screened 1163 MOFs for both adsorption and diffusion of CO_2 and

N_2. They also used UFF to describe Van der Waals interactions in classical simulation. Further, Keskin and co-workers[79-80] performed a large screening of MOFs using UFF with respect to the adsorption-based and membrane-based separation of CO_2/H_2 mixture plus the membrane-based separation of H_2/CH_4 mixture. There are also some studies that use Dreiding in molecular simulation for CH_4/H_2[81] separation and CO_2 capture for large scale-computational screening.[82]

Some studies used the generic force fields other than Dreiding and UFF. Yang and Zhong carried out a molecular simulation employing OPLS force field to present separation characteristic of CuBTC and MOF-5 for CO_2, CH_4, and H_2 adsorption.[27] Yang and colleagues[83] tried to elucidate the effect of electrostatic interactions on the adsorption of CO_2 in nine different MOFs. They used OPLS force field, and the results of simulation matched with experiment. Noguchi et al.[84] investigated quantum sieving effect defining interactions between H_2 and CuBOTf by OPLS. Another example of generic force field is AMBER. Wongsinlatam and Remsungnen[85] took both bonded and non-bonded interactions into account to observe the behavior of flexible MOFs using AMBER force field for all interactions except electrostatic interaction. They concluded that the results from rigid and flexible MOFs are similar.

The studies in the literature that examined the separation performance of MOFs are presented so far. These studies are performed with classical molecular simulation using generic force fields to define the Van der Waals interactions between adsorbate and adsorbent molecules. Accuracy of the force field directly affects the result of the simulation. Most of the molecular simulation studies in the literature investigated the accuracy of the force fields by means of comparison with experimental data.

There are various studies that compared the results of molecular simulation employing mostly UFF and Dreiding since they are widely used. For example, Perez-Pellitero[86] et al. studied CH_4 adsorption in ZIF-8 with UFF and Dreiding. They showed that the experimental adsorption values are close to the ones obtained with UFF and

Dreiding, and there is a better agreement with Dreiding compared to UFF. Keskin[87] compared the results of a simulation conducted using UFF and Dreiding with the experimental data for CO_2, H_2, and CH_4 adsorption in CU-TDPAT, and the simulation results highly matched with the experimental ones. Some studies demonstrated relatively low concordance with the experiment for adsorption of CO_2 in ZIF-68[88], and H_2 in IRMOF-1 and MOF-74.[89] Other force fields have also been compared, and the results confirmed the experimental data. Gee[90], Chen[59], Zhang[61] and their co-workers reported the molecular simulation results with AMBER/Dreiding, UFF/Dreiding/OPLS, AMBER/UFF/Dreiding, respectively. They compared simulation results with experimental ones for adsorption of CH_4 and C_2H_5OH in ZIF-8 and ZIF-90, CH_4 in CuBTC, and CH_4 in ZIF-8, respectively. Boyd et al.[91] recently evaluated the bulk properties of several MOFs using generic FFs and showed that UFF and Dreiding provide good values for the bulk modulus and linear thermal expansion coefficients of these materials. It is concluded that the results from generic force fields generally offer a good picture on the implementation for MOFs.

In the literature, there are many studies to investigate the accuracy of generic force fields by means of experimental data. However, the impact of FF type on the predicted gas separation performances of MOF adsorbents and their rankings has not been explored to date. Considering the ongoing research on high-throughput molecular simulations of MOFs for adsorption and separation of various gas mixtures, it is important to examine the robustness of ranking of MOF adsorbents with respect to the FF type. Driven with this point of view, the results of molecular simulation employing UFF and Dreiding were compared in Chapter 4 of this thesis. Adsorption data of 100 different MOF for CO_2/H_2, CO_2/N_2, and CO_2/CH_4 mixture was computed using both UFF and Dreiding. Results for UFF and Dreiding were evaluated with respect to four adsorbent selection metrics, which are adsorption selectivity, working capacity, adsorbent performance score (APS), and regenerability, in order to understand the effect of FF type. Then, how the selection of FF

type affects the ranking of material in terms of relevant performance metrics was investigated. The similarity of ranking list for UFF-based and Dreiding-based simulations was examined. At that point, it is important to note that it was not an intention to examine the accuracy of these FFs. It was aimed to define “a safe region” for MOFs in which using either Dreiding or UFF will not lead to significantly different results about the gas separation performance of a material. With this motivation, a force field factor depending on the number and type of the atoms present in the MOF was proposed and their corresponding energy parameters. It was showed that if this easily computable factor is low, then either Dreiding or UFF can be used to estimate the CO_2 uptake and CO_2 separation performance of the MOF. This factor will be highly useful to guide the simulators about the sensitivity of the predictions for the CO_2 uptake of MOFs to the FF type prior to performing computationally demanding molecular simulations.

Chapter 3

Computational Details

3.1 Selection of MOFs

We considered the same 100 MOFs that were studied in our previous work[92] to have a representative structural database that span a wide range of chemical functionalities. Our work took the 68 of 100 MOFs from the computation-ready database which was presented by Chung et al.[93] The remaining ones were taken from our other study.[94] Crystal structures of all MOFs were obtained from the Cambridge Crystallographic Data Centre (CCDC).[95] Zeo++ software[96] was used to compute the structural properties: pore volumes, densities, surface areas, limiting pore diameters (LPDs) and the largest cavity diameters (LCDs) of MOFs. The number of trials was set to 2000 (50000) and the probe size was set to 1.86 (0) Å for surface area calculations. When Zeo++ software was not able to compute the surface area and/or pore volume, Sarkisov and Harrison's algorithm, Poreblazer,[97] was used. The complete list of the materials with CCDC names and structural properties was displayed in Appendix A.

While He atom's sigma, He atom's epsilon, and N atom's sigma were set to 2.58 Å, 10.22 K, and 3.314 Å, the temperature, cut-off distance and number of trials were set to 298 K, 12.8 Å and 500, respectively. The largest anticipated pore diameter was set to 20 Å and the size of the bin was set to 0.25 Å.

3.2 Grand Canonical Monte Carlo (GCMC) Simulations

In Monte Carlo simulations, random infinite number of ensembles from a system is generated with probability, and the average behavior of ensembles gives the system

behavior. The ensemble can be any interest whose probability distribution is determined. Grand-canonical ensemble (μ, V, T) of a macroscopic system with MC technique is used to predict average particles in the system. At equilibrium, chemical potential (μ) and temperature (T) of gas are equal inside and outside of the adsorbent. We can think of a reservoir as shown in Figure 3.1 which contains adsorbent and gas, and imposes constant chemical potential and temperature. However, the particles and energy fluctuate with respect to configurations. A set of motion is required to define the configuration: translation, rotation, insertion, deletion and exchange of molecules. Adsorbed gas particles were calculated by specifying pressure, temperature and composition of the bulk gas mixtures. Pressure is calculated from chemical potential by equation of state.

We need partition function to apply the GCMC for a macroscopic system of interacting N particle in V volume, M-N ideal gas molecules in volume V_0-V can be written for grand-canonical ensemble as follows:[20]

$$\Omega(N, M, V, V_0, T)=\frac{V^N(V_0-V)^{M-N}}{\Lambda^{3M}N!(M-N)!}\int ds^{M-N}\int ds^N e^{-\beta U(S^N)} \quad (1)$$

where s^N is the reduced coordinates (fractional coordinates). Λ is the thermal de Broglie wavelength which equals $\sqrt{h^2/(2\pi m k_B T)}$. k_B, h and m denote the Boltzmann constant, Planck constant, and the mass of a gas atom, respectively.

M-N particles in volume V_0-V exchange with N particles in volume V as shown in Figure 3.1. In volume V, the particles can interact each other but not in volume V_0-V. If a molecule moves from volume V_0-V to V, the potential energy changes from $U(s^N)$ to $U(s^{N+1})$.

For M particles over two separate volumes, the total partition function is then given in Equation (2):[20]

$$\Omega(M, V, V_0, T)=\sum_{N=0}^{M} \frac{V^N(V_0-V)^{M-N}}{\Lambda^{3M}N!(M-N)!}\int ds^{M-N}\int ds^N e^{-\beta U(S^N)} \quad (2)$$

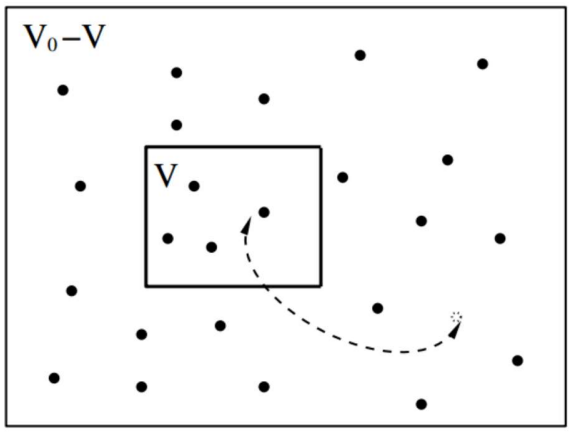

Figure 3.1. The schematic display of movement of exchange[20]

Acceptance rules are applied for trial moves including particle displacement, particle insertion and deletion in GCMC simulations. The probability of particle displacement, particle insertion and deletion are given in Equations (3), (4), and (5), respectively.

$$acc(s\rightarrow s')=\min\left[1, \exp\left\{-\beta\left(U(s'^N)-U(s^N)\right)\right\}\right] \quad (3)$$

$$acc(N\rightarrow N+1)=\min\left[1, \frac{V}{\Lambda^3(N+1)}\exp\{\beta[\mu-U(N+1)+U(N)]\}\right] \quad (4)$$

$$acc(N\rightarrow N-1)=\min\left[1, \frac{\Lambda^3 N}{V}\exp\{-\beta[\mu+U(N-1)-U(N)]\}\right] \quad (5)$$

The configurational energy, pressure and density of ensemble are averaged as the corresponding properties of the system. The average number of molecules adsorbed on MOF calculated from Equation (6) from GCMC simulations. [20]

$$\langle N\rangle = kT\left(\frac{\partial \ln \Omega}{\partial \mu}\right) \tag{6}$$

Intermolecular and intramolecular interactions are calculated for each configuration as the system energy in GCMC simulations. The energy of the system is calculated as sum of these components: [34]

$$E = \sum E_s + \sum E_b + \sum E_t + \sum E_{oop} + \sum E_{el} + \sum E_{vdW} \left(+ \sum E_{other}\right) \tag{7}$$

where the first four terms are stretching, bending, torsional, and inversion potentials, respectively which are the bonded interactions between the atoms of gas molecule and MOF themselves. We did not take account the intramolecular forces and assumed the gas molecule and MOF as rigid. Other three terms are non-bonded interactions: Van der Waals, electrostatic interactions and others While Van der Waals energy consists of the short-range repulsive exchange potential and the attraction due to London dispersion, the electrostatic interaction is the result of the atomic partial charge of adsorbent atoms and the polarity of adsorbate.[33-34] Other interaction is generally hydrogen binding.

We defined intermolecular interactions using Lennard-Jones (12-6)[98] potentials for both MOFs and gas molecules as shown in Equation (8).

$$U_{LJ} = 4\varepsilon_{ij}\left[\left(\frac{\sigma_{ij}}{r_{ij}}\right)^{12} - \left(\frac{\sigma_{ij}}{r_{ij}}\right)^{6}\right] \tag{8}$$

where σ and ε represent, kinetic size (Å) and the energy parameter (K), respectively. U_{LJ} is the interatomic potential between the i and j atoms, and r_{ij} is the distance between the i and

j atoms. Three-site rigid molecule with LJ 12-6 potential was used to model CO_2, and the locations of the partial point charges were set as the center of each site.[99] N_2 was also modeled as three-site molecule; two sites were located at the N atoms and the third site was located at the center of the mass with partial point charges.[100] H_2[101] and CH_4[102] were modeled by using single-site spherical LJ 12-6 potential. For MOFs, two cases were investigated. Firstly, the molecular simulation was performed taking LJ 12-6 potentials from Dreiding and then repeated under the same conditions using the potentials from UFF. For some metal atoms of the MOFs, such as Ag, Be, Cd, Co, Cu, Fe, Mn, Nd, Ni, Zr, potential parameters are not available in the Dreiding FF. These parameters were taken from the UFF for both cases. The Lorentz-Berthelot mixing rules were employed.[32] The cut-off distance for truncation of the intermolecular interactions was set to 13 Å. Electrostatic interactions were taken into consideration using the Coulomb potential as given in Equation (9) for the gas molecules with multipole moments, CO_2, and N_2.

$$U_{ij} = \frac{1}{4\pi\varepsilon_0}\frac{q_i q_j}{r_{ij}} \quad (9)$$

where q_i and q_j represent the partial atomic charges of i and j atoms, respectively, and ε_0 is the electric constant which is also known as the absolute permittivity of free space. The cut-off distance for truncation of electrostatic interactions was set to 25 Å. In order to compute the electrostatic interactions between gas molecules and MOFs, partial point charges were assigned to MOF atoms using extended charge equilibration method (EQeq).[103] A recent study examined the impact of atomic charge assignment methods of MOFs on the high-throughput computational screening for CO_2/H_2O separations and found that majority of the top MOFs are identical regardless of the charge assignment method.[104]

GCMC simulations were performed to compute adsorption isotherms of binary gas mixtures, such as CO_2/H_2, CO_2/N_2, CO_2/CH_4 in MOFs. Periodic boundary conditions were applied in all simulations. A simulation box of 2×2×2 crystallographic unit cells was

used. During the simulations, 1.5×10^7 steps were performed to guarantee the equilibration and 1.5×10^7 steps were performed to sample the desired properties. Rigid framework assumption was used in all simulations following the literature,[86, 105-106] and the good agreement between the results of simulations using rigid framework and the experimentally measured gas adsorption data was shown in our previous work.[92]

3.3 Generic Force Fields

These two FFs are widely used in the simulations of MOFs for gas adsorption because they offer the advantage of being adaptable to many chemical environments. Dreiding is a generic FF developed back in 1990 to predict structures and dynamics of organic, biological, and main group inorganic molecules.[28] UFF was introduced in 1992 as a full periodic table FF where the parameters were estimated using general rules based on the element itself, its hybridization and its connectivity.[29] The force field is calculated as the sum of bonded (valance) and non-bonded interactions:

$$E=E_{bonded}+E_{non\text{-}bonded} \quad (10)$$

The bonded interactions consist of same bonded interaction terms for both Dreiding and UFF derivation as shown in Equation (11):

$$E_{bonded}=E_{stretch}+E_{angle}+E_{torsion}+E_{inversion} \quad (11)$$

where first term is the bond stretching of two-body, second term is bond angle bend for three-body, and third and fourth terms are dihedral angle torsion and inversion term for four-body, respectively.

The bonded interactions are slightly different for Dreiding and UFF. While Dreiding calculates non-bonded interactions as sum of van der Waals interaction and electrostatic interactions, UFF also includes hydrogen bonding energy.

$$E_{non\text{-}bonded}=E_{VdW}+E_{electrostatic}+E_{hydrogen\ bonding}\ (\text{in UFF}) \quad (12)$$

Dreiding and UFF use exactly same expression for van der Waals and electrostatic interactions with same combining rules. They utilize LJ 12-6 and Coulomb interactions to describe these interactions. They also explored different types of potential expression for the components of both bonded and non-bonded interactions.

3.4 Calculating Adsorbent Properties of MOFs

Adsorption data of gas mixtures obtained from the GCMC simulations were used to compute several adsorbent evaluation metrics, namely adsorption selectivity (S), working capacity (ΔN),[107] sorbent selection parameter (S_{sp}),[108] and per cent regenerability (R%). Calculation details of these metrics are given in Table 3.1.

Table 3.1. Adsorbent evaluation metrics used in ranking of MOFs.

Metrics	Calculation
Selectivity	$S_{ads(1/2)}=\frac{x_1/x_2}{y_1/y_2}$
Working capacity (mol/kg)	$\Delta N=N_{ads}-N_{des}$
Sorbent selection parameter	$S_{sp}=\frac{(S_{ads(1/2)})^2}{(S_{des(1/2)})}\times\frac{\Delta N_1}{\Delta N_2}$
Per cent regenerability (%)	$R\%=\frac{\Delta N_1}{N_{1,ads}}\times 100\ \%$
APS (mol/kg)	$APS=S_{ads(1/2)}\times\Delta N_1$

In these equations, x (y) represents the compositions of the adsorbed (bulk) gases in the adsorbent, N_{ads} and N_{des} are the gas uptakes at the adsorption and desorption pressures, respectively. Subscript 1 (2) represents strongly (weakly) adsorbed gas. In our study, the component 1 is always CO_2, and the component 2 is H_2, N_2 or CH_4 depending on the mixture. All calculations were performed at the adsorption pressure of 1 bar and the desorption pressure of 0.1 bar at 298 K. Compositions of the binary gas mixtures were set as CO_2/H_2:15/85, CO_2/N_2:15/85, and CO_2/CH_4:50/50 in molecular simulations in order to mimic industrial operating conditions.

Chapter 4

Effects of Force Field Selection on the Computational Ranking of MOFs for CO_2 Separations*

Selectivity is generally considered as the primary metric in ranking adsorbent materials. An adsorbent with high selectivity is accepted as promising in gas separation applications. Therefore, selectivities of MOFs for CO_2/H_2, CO_2/N_2, and CO_2/CH_4 mixtures were firstly computed at 1 bar and 298 K using the mixture adsorption data obtained from the GCMC simulations. The CO_2 selectivities of MOFs computed from molecular simulations employing Dreiding and UFF are compared in Figure 4.1 for three gas mixtures. Comparison of selectivities obtained from two sets of molecular simulations using different FFs is also separately given for CO_2/H_2, CO_2/N_2, and CO_2/CH_4 mixtures in Figure B2, B3, B4, respectively.

The CO_2 selectivities calculated with Dreiding (UFF) are in the ranges of 10.48−2237.35 (12.38−3119.09), 3.73−202.30 (3.75−197.48), and 1.66−59.38 (1.71−60.97) for CO_2/H_2, CO_2/N_2, and CO_2/CH_4 mixtures, respectively. Figure 4.1 shows that molecular simulations with UFF led to slightly higher selectivities for CO_2/H_2 mixtures compared to the ones with Dreiding. Selectivities calculated for CO_2/N_2 and CO_2/CH_4 mixtures were similar for most MOFs regardless of the FF type. In extreme cases, using UFF can give 2.2, 1.6, and 1.7 times larger CO_2/H_2, CO_2/N_2, and CO_2/CH_4 selectivities than using the Dreiding FF. For example, CO_2/H_2 selectivity of a MOF,

* The results given in this chapter were published in Industrial & Engineering Chemistry Research with following reference: Dokur, D. and Keskin, S. (2018) "Effects of Force Field Selection on the Computational Ranking of MOFs for CO_2 Separations" Ind. Eng. Chem. Res. 2018, 57, 2298−2309. The original manuscript has been rearranged to conform to the format requirements of the dissertation.

LASPOM, was predicted as 205.59 by Dreiding and 441.25 by UFF, leading to a large difference of 114.63%. The largest deviations for CO_2/N_2 and CO_2/CH_4 selectivities were observed for OCIZIL and LUXDEO, respectively. The CO_2/N_2 (CO_2/CH_4) selectivity of the relevant MOF was predicted as 47.00 (8.45) by Dreiding and 75.10 (14.54) by UFF, resulting in 59.77% (71.97%) difference. The discrepancies originated from using different FFs can be explained with the changes in the energy parameters of MOF atoms 114.63%.

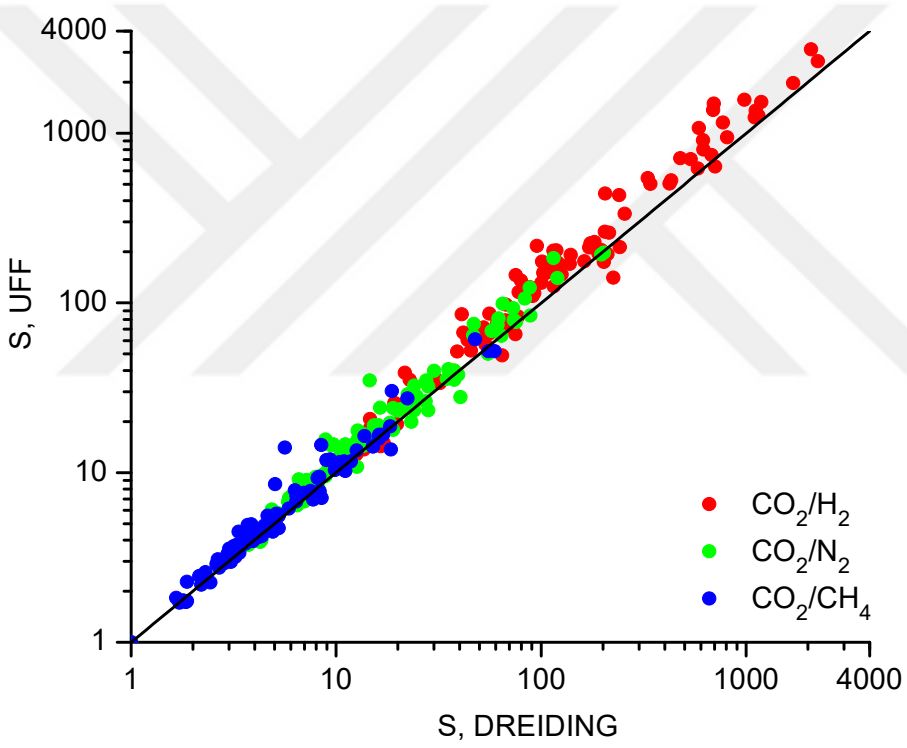

Figure 4.1. Comparison of selectivities of MOFs computed using Dreiding and UFF for CO_2/H_2, CO_2/N_2, CO_2/CH_4 separations. Diagonal line is to guide the eye.

The largest deviations for CO_2/N_2 and CO_2/CH_4 selectivities were observed for OCIZIL and LUXDEO, respectively. The CO_2/N_2 (CO_2/CH_4) selectivity of the relevant MOF was predicted as 47.00 (8.45) by Dreiding and 75.10 (14.54) by UFF, resulting in 59.77% (71.97%) difference. The discrepancies originated from using different FFs can be explained with the changes in the energy parameters of MOF atoms. For example, OCIZIL has Zn as the metal atom and the energy parameter of Zn significantly increases when the UFF was used instead of Dreiding ($\varepsilon_{Zn,Dreiding}/k_B$ = 27.69 K, $\varepsilon_{Zn,UFF}/k_B$ =62.44 K) in simulations. As a result, adsorption of CO_2 increases and more pronounced deviations are observed for the CO_2 selectivity. Overall, Figure 4.1 shows that both Dreiding and UFF can be used in the molecular simulations for the initial screening of MOF adsorbents based on selectivity, however caution is advised especially for CO_2/H_2 mixtures where the selectivity predictions of Dreiding and UFF may significantly vary. At that point, it is important to note that the MOFs considered in this thesis have metal atoms of Ag, Al, Be, Cd, Co, Cu, Fe, In, Mn, Nd, Ni, V, Zn, and Zr. Among these, Al, In, and Zn have different energy parameters in Dreiding and UFF. The change in the energy parameters of Zn is the highest as can be seen in Table B1. For example, the energy parameters of In in the UFF and Dreiding are very close ($\varepsilon_{In,Dreiding}/k_B$ = 276.96 K, $\varepsilon_{In,UFF}/k_B$ = 301.63 K). Although there are changes in the energy parameters, the correlation coefficients (R^2) between the predictions of Dreiding and UFF for the selectivities of MOFs containing Al, In, and Zn were computed to be not very different (0.97, 0.95, and 0.89 for CO_2/H_2, CO_2/N_2, and CO_2/CH_4 mixtures, respectively) than the R^2 values (0.96, 0.94, and 0.94 for CO_2/H_2, CO_2/N_2, and CO_2 /CH_4 mixtures, respectively) computed for MOFs that contain other metals.

Since selectivity solely depends on the gas uptakes of MOFs, the role of the FF type on the gas uptakes of MOFs were examined. Among the four gases considered, CO_2 is the most strongly adsorbed component. It was represented as a three-site molecule which has more interactions sites with the MOF atoms compared to other gases in addition to the

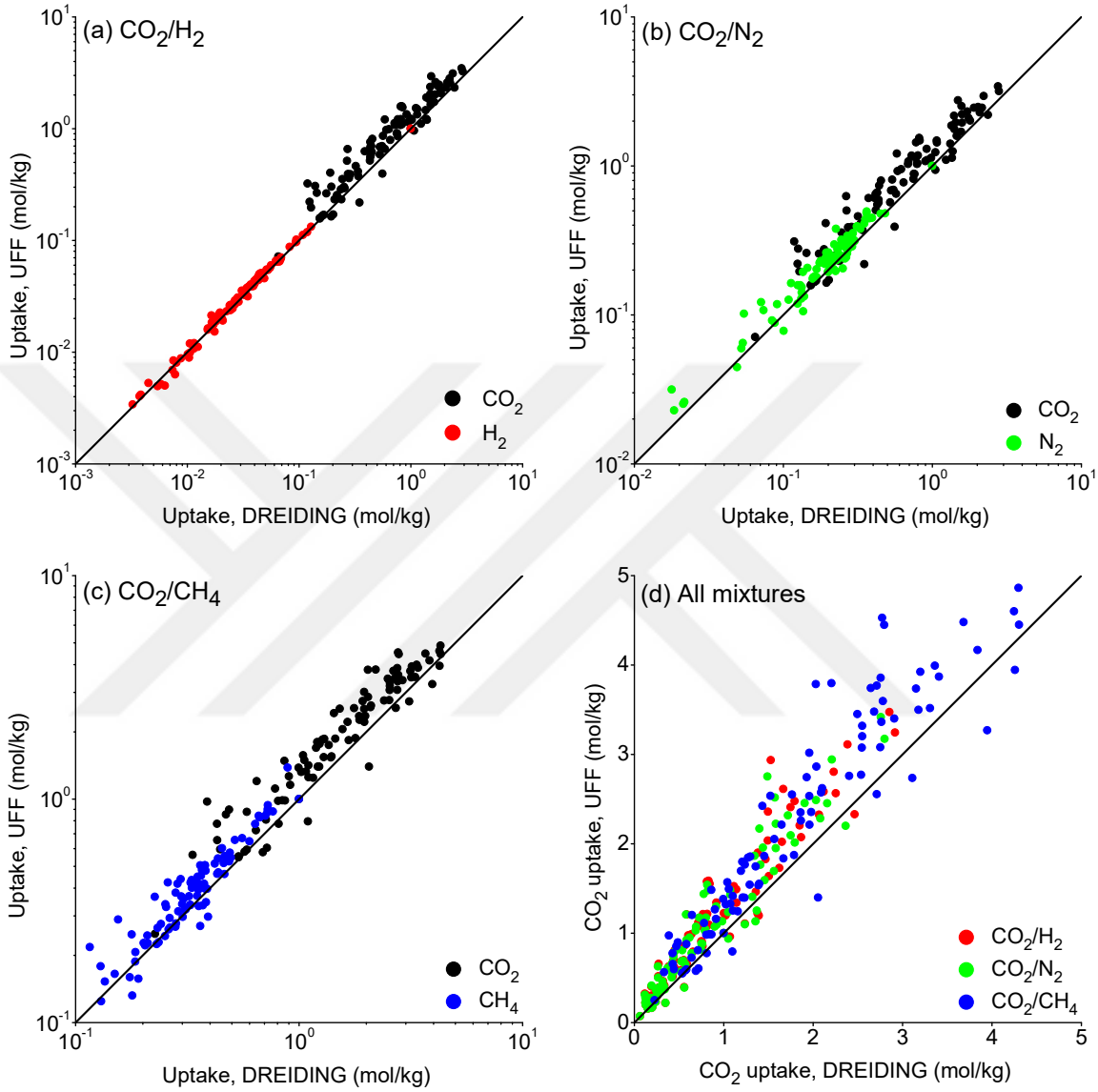

Figure 4.2. Comparison of gas uptakes of MOFs computed using Dreiding and UFF for (a) CO_2/H_2, (b) CO_2/N_2, (c) CO_2/CH_4, (d) all mixtures. Diagonal lines are to guide the eye.

electrostatic interactions due to its quadrupole moment. H_2 has very weak interactions with MOFs leading to very low uptakes. Figure 4.2 shows that molecular simulations performed at 1 bar using UFF generally result in higher uptakes for CO_2, CH_4 and N_2 compared to the ones performed using Dreiding. This result is more pronounced for CO_2, followed by CH_4 and N_2, as can be seen in Figure B5, B6, and B7 where uptakes for each gas species are separately shown.

The CO_2 uptakes of MOFs for CO_2/H_2, CO_2/N_2, and CO_2/CH_4 mixtures were computed as 0.07−2.92 (0.07−3.47), 0.06−2.80 (0.07−3.42), and 0.23−4.30 (0.25− 4.86) mol/kg, respectively using the Dreiding (UFF).The H_2 uptakes of MOFs were calculated to be almost same, 0.003− 0.13 mol/kg, regardless of the FF type. The correlation coefficient (R^2) was defined as a linear fit between the Dreiding predicted results and UFF predicted results. The R^2 between the predictions of Dreiding and UFF for the gas uptakes of MOFs computed at 1 bar are given in Table 4.1. The R^2 values also show that CO_2 is the component which is more sensitive to the FF type, followed by N_2 and CH_4, whereas H_2 uptakes do not change with the FF.

Table 4.1. Correlation coefficients (R^2) for the gas uptakes predicted by Dreiding and UFF.

	CO_2 uptake (mol/kg)		**H_2 uptake (mol/kg)**		**N_2 uptake (mol/kg)**		**CH_4 uptake (mol/kg)**	
	0.1 bar	1 bar	0.1 bar	1 bar	0.1 bar	1 bar	0.1 bar	1 bar
CO_2/H_2	0.9419	0.9177	0.9914	0.9952	-	-	-	-
CO_2/N_2	0.9403	0.9179	-	-	0.9268	0.9136	-	-
CO_2/CH_4	0.9408	0.8813	-	-	-	-	0.8404	0.9293

Since UFF-based simulations overpredicted the N_2 and CH_4 uptakes of MOFs in similar amounts compared to the CO_2 uptake, CO_2/N_2 and CO_2/CH_4 selectivities predicted

by two FFs were not significantly different as previously shown in Figure 4.1. The CO_2 uptakes predicted by UFF were higher than those of Dreiding but almost same for H_2. As a result, UFF-based simulations give much larger CO_2/H_2 selectivities than those of the Dreiding based ones. These results indicate that the more strongly adsorbed component in MOFs, in this case CO_2, is more sensitive to the type of the FF used in the simulations compared to the weakly adsorbed gases. In other words, if the adsorption competition between two gas molecules is low, such as CO_2 and H_2, then selectivities predicted by two different FFs can be significantly different.

Working capacity is generally considered as the second most important metric used to evaluate new adsorbent materials. Figure 4.3 represents the predicted CO_2 working capacities of MOFs at an adsorption pressure of 1 bar and desorption pressure of 0.1 bar. Detailed comparison of CO_2 uptakes of MOFs at 0.1 and 1 bar using Dreiding and UFF can be found in Figure B8, B9, and B10 for all three mixtures. Similar to the CO_2 uptakes, CO_2 working capacities predicted by UFF generally overestimated the predictions of Dreiding. Table 4.2 shows that R^2 values of the working capacities (0.86−0.89) are lower than those of selectivities (0.94−0.95), indicating that working capacity is much more sensitive to the FF type than the selectivity.

Table 4.2. Correlation coefficients (R^2) for the performance evaluation metrics predicted by Dreiding and UFF for each gas mixture.

	S	**ΔN_{CO2} (mol/kg)**	**S_{sp}**	**R%**
CO_2/H_2	0.9528	0.8928	0.9674	0.9378
CO_2/N_2	0.9434	0.8936	0.9552	0.9377
CO_2/CH_4	0.9408	0.8648	0.9105	0.9549

Combining selectivity and working capacity in a single parameter, S_{sp} is useful to easily identify the most promising adsorbents. S_{sp} values of MOFs were compared using

the results of simulations employing Dreiding and UFF in Figure 4.4. The S_{sp} values of MOFs for CO_2/H_2, CO_2/N_2, and CO_2/CH_4 separations were calculated as 19.34−3.9 × 10^5 (26.74−6.9 × 10^5), 2.51−5178.36 (2.54−8980.72), and 2.91− 2276.69 (3.02−1.07 × 10^4), respectively using the Dreiding (UFF). These numbers indicate that quantitative predictions of molecular simulations for S_{sp} strongly depend on the FF type.

This is in fact a natural result of the mathematical description of S_{sp}. It includes the square of the selectivity, and as discussed in Figure 4.1, there are several MOFs for which UFF-based simulations predicted double of the CO_2 selectivities compared to the Dreiding-based simulations.

As a result, there are MOFs for which using UFF gives 1.73, 1.73, and 4.70 times higher S_{sp} values than using Dreiding for CO_2/H_2, CO_2/N_2, and CO_2/CH_4 separations, respectively.

The impact of FF on the predicted percent regenerabilities (R%) of MOFs was examined. Although MOF adsorbents are used to be ranked based on selectivity, our recent study showed that it is much more efficient to screen MOFs based on R% because a large number of MOFs having high CO_2 selectivities suffers from very low R% (<75%).[92] Figure 4.5 shows that R% of MOFs ranges from 48.83 to 90.64% (44.32−91.12%) for CO_2/H_2 separation based on the molecular simulations performed using Dreiding (UFF). R% is defined as the ratio of working capacity to the gas uptake at an adsorption pressure. Since overestimation of UFF for CO_2 uptake is higher than the one for the CO_2 working capacity, R% predictions of UFF are generally lower than those of Dreiding. R% of MOFs ranges from 46.32 to 90.47% (33.52−91.48%) for CO_2/N_2 (CO_2/CH_4) separation based on the molecular simulations performed using Dreiding whereas UFF results are slightly less, 44.39−90.83% (26.37−91.68%). Similar to the selectivity, the R^2 values for R% (0.94−0.95) are high, as shown in Table 4.2, although sometimes large quantitative deviations were observed in the predicted R% values from two different FFs.

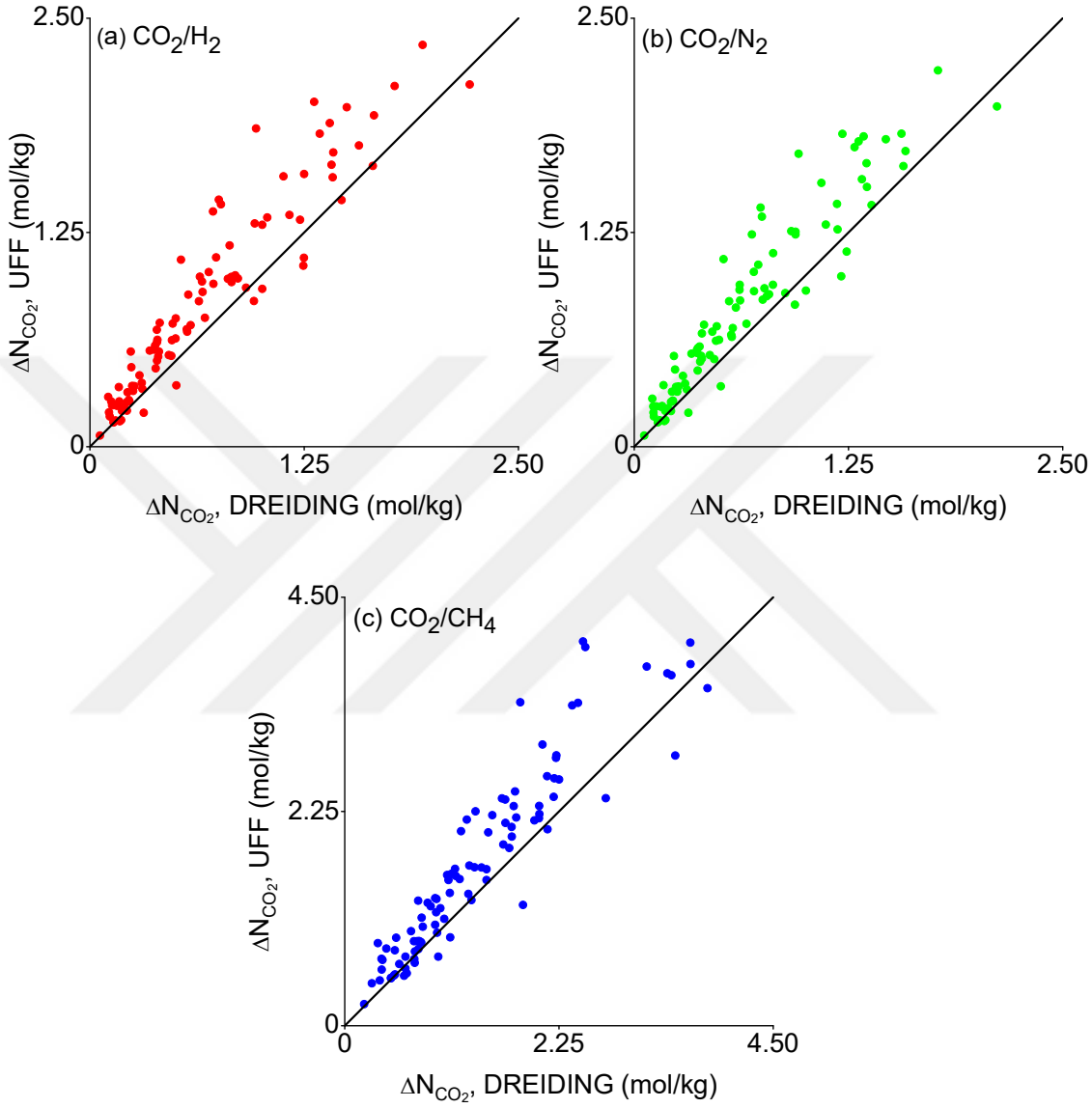

Figure 4.3. Comparison of the CO_2 working capacities of MOFs computed using Dreiding and UFF for (a) CO_2/H_2, (b) CO_2/N_2, (c) CO_2/CH_4 mixtures. Diagonal lines are to guide the eye.

R^2 values calculated for all the adsorbent evaluation metrics can be seen in Table 4.2. The R^2 values are high (>0.86) for all four metrics suggesting that both FFs make quantitatively similar estimates for the four performance evaluation metrics discussed. Therefore, how the rankings of best MOF adsorbents change with Dreiding and UFF were examined. The top 10 MOFs rankings based on the four performance evaluation metrics computed from two different FFs are listed in Table 4.3.

According to the CO_2/H_2 selectivity ranking, there are 8 common MOFs in the top promising material lists of Dreiding and UFF. Ranking of the materials is very similar. For example, EMIVAY, EYOQAL, and BERGAI01 are identified as the top three selective MOFs based on the Dreiding. EYOQAL is the first, EMIVAY is the second, and BERGAI01 is the third MOF in the selectivity ranking of UFF-based simulations. Similarly, 8 MOFs are common in the promising material list for CO_2/N_2 separation. Ranking of the first 4 MOFs is very similar in both lists. For instance, KEYFIF01 and KEYFIF are the first and the second materials in both rankings. The third and fourth MOFs, EMIVAY and EYOQAL, identified based on the Dreiding only change their places as the fourth and third in the UFF-based list. All MOFs except one are the same in CO_2/CH_4 selectivity rankings. Rankings of top 5 MOFs for CO_2/CH_4 selectivity are very similar. For instance, KEYFIF has the second highest selectivity in both lists. The first and the third MOFs according to Dreiding results are KEYFIF01 and GIWNUV, and they are the third and first MOF, respectively, in the UFF-based list. The numbers of identical MOFs in top 10 rankings based on molecular simulations employing different FFs are also tabulated in Table B2. The high numbers of common MOFs that appear in both lists indicate that Dreiding and UFF predict similar selectivity ranking of MOFs, supporting the further use of these two generic FFs in high-throughput screening studies to identify the most selective adsorbents for CO_2 separations.

Table 4.3. Top 10 MOFs for CO_2/H_2, CO_2/N_2, and CO_2/CH_4 separations based on the performance evaluation metrics computed using Dreiding or UFF in the molecular simulations.

DREIDING								UFF							
S		**ΔN (mol/kg)**		**Ssp**		**R (%)**		**S**		**ΔN (mol/kg)**		**Ssp**		**R (%)**	
CO_2/H_2															
EMIVAY	2237.35	EMIHAK	2.22	EYOQAL	399712.29	GALBUS	90.64	EYOQAL	3119.09	HAJKOU	2.34	EYOQAL	689817.90	GALBUS	91.12
EYOQAL	2074.29	HAJKOU	1.94	EMIVAY	320862.42	IDIWOH	90.53	EMIVAY	2657.41	EMIHAK	2.11	EMIVAY	396894.35	DIDBID	90.89
BERGAI01	1692.67	EYOPOY	1.78	BERGAI01	204453.75	LECQEQ	90.52	BERGAI01	1977.81	EYOPOY	2.10	OCIZIL	275032.38	DIDBOJ	90.81
EYOPUE	1185.13	AJIHOQ	1.66	EMIHAK	153268.06	DIDBID	90.45	BOWSIQ	1574.21	ACODED	2.01	BERGAI01	267405.19	EMIHAK	90.72
KEYFIF01	1145.27	EYOQAL	1.65	KEYFIF01	124385.74	WOBHIF	90.38	EYOPUE	1526.30	HAJKIO	1.98	BOWSIQ	247581.23	IDIWOH	90.65
QIFLOI	1115.11	RAYLIO	1.57	KEYFIF	115796.15	DIDBOJ	90.34	LUXDEO	1492.43	AJIHOQ	1.93	HAJKOU	239714.86	HASSUR	90.47
KEYFIF	1102.57	HAJKIO	1.50	HAJKOU	113261.26	LARVIL	90.32	OCIZIL	1371.82	DEJROB	1.89	QIFLOI	200871.41	LARVIL	90.42
BOWSIQ	979.93	EMIVAY	1.47	QIFLOI	104208.24	KUGZIW	90.32	QIFLOI	1354.35	LUXDEO	1.86	LUXDEO	190800.84	KUGZIW	90.36
PEQHOK	808.73	NUTQEZ	1.42	BOWSIQ	87513.61	OWIVEW	90.29	KEYFIF01	1272.47	NEFTOJ	1.83	EBEMOO	163889.32	LUKLIN	90.31
HAJKOU	769.15	RAYLOU	1.42	OCIZIL	86404.58	HECQUB	90.27	KEYFIF	1237.20	RAYLIO	1.76	KEYFIF01	153588.38	LECQEQ	90.31
CO_2/N_2															
KEYFIF01	202.30	EMIHAK	2.12	KEYFIF01	5178.36	IDIWOH	90.47	KEYFIF01	197.48	HAJKOU	2.19	EYOQAL	8980.72	LECQEQ	90.83
KEYFIF	196.58	HAJKOU	1.77	KEYFIF	4875.75	LARVIL	90.44	KEYFIF	192.48	EMIHAK	1.98	KEYFIF01	4538.97	GALBUS	90.71
EMIVAY	119.89	RAYLIO	1.58	EYOQAL	2364.93	GALBUS	90.42	EYOQAL	183.24	AJIHOQ	1.83	KEYFIF	4415.73	DIDBID	90.62
EYOQAL	114.87	EYOQAL	1.57	EMIVAY	1410.22	LECQEQ	90.38	EMIVAY	140.05	ACODED	1.82	EMIVAY	2375.10	WOBHIF	90.50
RAYLIO	88.62	AJIHOQ	1.56	BERGAI01	1065.31	OWIVEW	90.31	BERGAI01	123.01	HAJKIO	1.81	BERGAI01	2276.71	IDIWOH	90.48
BERGAI01	88.05	EYOPOY	1.47	EMIHAK	933.91	DIDBOJ	90.30	EYOPUE	105.87	EYOPOY	1.79	LUXDEO	1634.31	DIDBOJ	90.43
EYOPUE	83.33	EMIVAY	1.38	RAYLIO	863.30	DIDBID	90.27	LUXDEO	98.70	DEJROB	1.78	OCIZIL	1265.47	LARVIL	90.40
QIFLOI	75.48	RAYLOU	1.36	QIFLOI	802.52	KUGZIW	90.24	BOWSIQ	92.95	NEFTOJ	1.75	HAJKOU	1247.89	KUGZIW	90.25
YOZBOF	73.58	NUTQEZ	1.36	EBEMOO	682.03	LUKLIN	90.22	RAYLIO	84.30	RAYLIO	1.72	QIFLOI	1120.95	HECQUB	90.23
BOWSIQ	73.17	HAJKIO	1.34	NUJCIE	656.31	OWITAQ	90.22	EBEMOO	80.76	LUXDEO	1.71	EBEMOO	1118.21	LUKLIN	90.21
CO_2/CH_4															
KEYFIF01	59.38	LECQEQ	3.81	KEYFIF01	2276.69	IDIWOH	91.48	GIWNUV	60.97	DIDBID	4.03	EYOQAL	10698.50	IDIWOH	91.68
KEYFIF	55.29	AJIHOQ	3.63	KEYFIF	1919.38	OWIVEW	91.12	KEYFIF	51.86	NUTQEZ	4.02	GIWNUV	1622.66	LARVIL	91.17
GIWNUV	47.61	NUTQEZ	3.63	GIWNUV	1247.37	KUGZIW	90.78	KEYFIF01	51.82	GALBUS	3.98	KEYFIF	1619.34	HECQUB	91.03
EYOPUE	22.29	FIQCEN	3.47	EYOQAL	509.95	WOBHIF	90.74	EYOQAL	30.22	AJIHOQ	3.80	KEYFIF01	1609.06	LUKLIN	90.73
EYOQAL	18.71	EMIHAK	3.43	EMIHAK	503.76	OWITAQ	90.73	EYOPUE	27.33	NEFTOJ	3.77	EYOPUE	987.38	OWIVEW	90.69
LARVIL	18.52	HASSUR	3.39	LARVIL	389.94	OWIVAS	90.72	RAYLIO	18.74	HASSUR	3.70	EMIHAK	600.43	OWIVAS	90.65
RAYLIO	18.39	NEFTOJ	3.17	EYOPUE	365.12	HECQUB	90.69	EMIHAK	16.72	EMIHAK	3.68	HAJKOU	510.59	OWITAQ	90.64
NUJCIE	16.93	EMIHIS	2.74	AJIHOQ	284.63	OWITOE	90.61	NUJCIE	16.69	LECQEQ	3.54	LUXDEO	462.51	OWITOE	90.59
EMIHAK	16.23	GALBUS	2.53	LECQEQ	252.81	LUKLIN	90.61	BOWSIQ	16.43	WOBHIF	3.40	AJIHOQ	371.08	OWITUK	90.58
EMIVAY	16.14	DIDBID	2.50	NUJCIE	232.24	OWITEU	90.57	EMIVAY	15.88	DIDBOJ	3.39	BOWSIQ	348.77	OWITEU	90.55

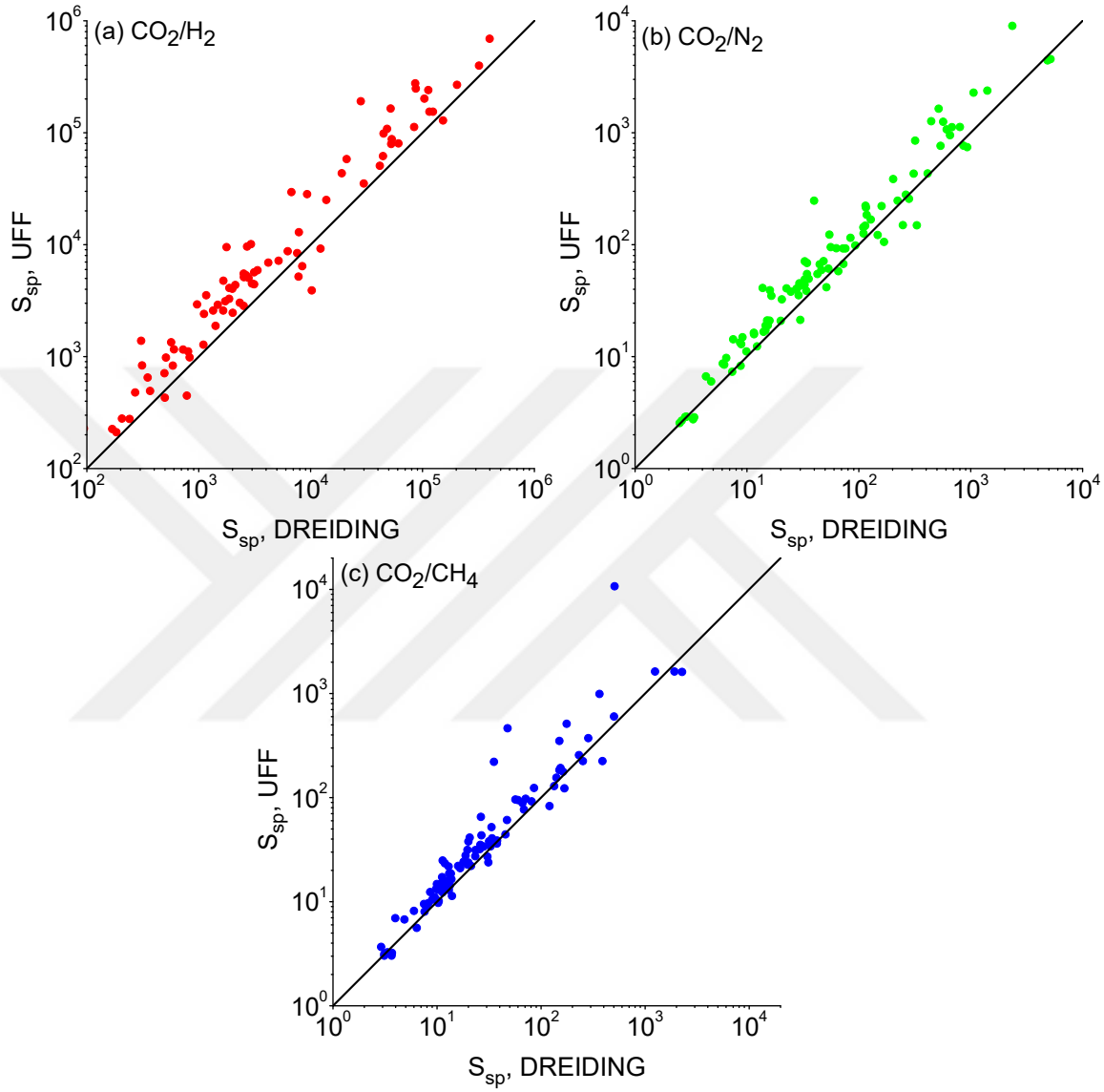

Figure 4.4. Comparison of sorbent selection parameters of MOFs computed using Dreiding and UFF for (a) CO_2/H_2, (b) CO_2/N_2, (c) CO_2/CH_4 mixtures. Diagonal lines are to guide the eye.

The most promising 10 MOFs based on the CO_2 working capacities are also given in Table 4.3. There are 6, 6, and 8 common MOFs in the Dreiding and UFF lists for CO_2/H_2, CO_2/N_2, and CO_2/CH_4 separations, respectively. Rankings of the top 3 MOFs are very similar for CO_2/H_2, and the top 2 MOFs are the same for CO_2/N_2. Although 8 MOFs are common in the list, their rankings are quite different for CO_2/CH_4 separation. For example, the tenth MOF in the list of Dreiding is the first MOF in the UFF list. This result supports the lowest R^2 value between the predicted performance metrics of Dreiding and UFF for the CO_2 working capacity of CO_2/CH_4 mixture as shown in Table 4.2. There are 8, 7, and 7 common MOFs in the Dreiding and UFF lists for S_{sp} rankings of MOFs for CO_2/H_2, CO_2/N_2, and CO_2/CH_4 separations, respectively. The First two MOFs for CO_2/H_2 mixture and top 5 (4) MOFs for CO_2/N_2 (CO_2/CH_4) mixture are the same in both lists. Here, it is important to note that although the S_{sp} rankings have many common MOFs, there are significant quantitative differences in S_{sp} values of the top promising MOFs identified by Dreiding and UFF. Seven out of the top 10 MOFs for regenerability ranking are identical for CO_2/H_2 separation. The top 3 MOFs identified in the Dreiding-based simulations rank as first, fifth, and tenth in the UFF-based list. Although 8 of the top 10 MOFs are common in both lists for CO_2/N_2 separation, their rankings are different. For example, the top 4 MOFs in the Dreiding-based list are fifth, seventh, second, and first in the list of UFF.

Finally, there are 8 identical MOFs in the regenerability lists for CO_2/CH_4 separations. The first, sixth, eighth, and tenth of the top 10 MOFs in the Dreiding list have the same rankings with the UFF list. Since these top MOFs have not been experimentally tested for CO_2 separations to the best of our knowledge, it is not able to make a comparison between experimentally measured and simulated performance evaluation metrics. The good agreement between experimentally measured and predicted CO_2/H_2, CO_2/N_2, and CO_2/CH_4 selectivities of various MOFs was shown in Figure B1, and it can

be accepted that our computational approach will make accurate estimates for the selectivities of MOFs which have not been experimentally tested yet.

In order to quantify the robustness of the ranking of MOFs to the FF selection, the Spearman's ranking correlation coefficients (SRCC) were also computed. Values of SRCC change from −1 to 1 and indicate the correlation between two sets of ranking lists. It was shown in Table B3 that SRCC is 0.98, 0.95, 0.97, and 0.96 for S, ΔN, S_{sp}, and R%, respectively.

This analysis suggests that the rankings of 100 MOFs based on the Dreiding FF are positively correlated with those based on the UFF, and strength of the correlation is very high. These results show that either of the generic FF can be safely used to screen and rank MOFs based on the four adsorbent performance evaluation metrics that considered in this thesis. Throughout the manuscript, our aim is not to show superiority/accuracy of one generic FF over another but to understand how the ranking of the best MOF adsorbents changes based on the FF type. Results show that adsorbent evaluation metrics quantitatively change due to the differences in the predicted CO_2 uptakes of MOFs depending on the FF. In order to provide a guideline for the simulators in selecting either Dreiding or UFF, a simple factor that assesses sensitivity of the CO_2 uptake to the FF type was proposed. With this factor, the aim is to differentiate between the MOFs for which using either Dreiding or UFF does not make any significant difference in the predicted CO_2 uptakes and the MOFs for which the type of the FF plays an important role in predicting the CO_2 uptakes and separation performance of the materials. The force field factor (FFF) was defined using the energy parameters of atoms in the Dreiding and UFF. Almost all atoms have different energy and size parameters (ε/k_B and σ, respectively) in each FF. For example, carbon is available in all MOFs, its ε and σ parameters are 47.89 K and 3.47 Å in Dreiding, whereas 52.87 K and 3.43 Å, respectively in the UFF.

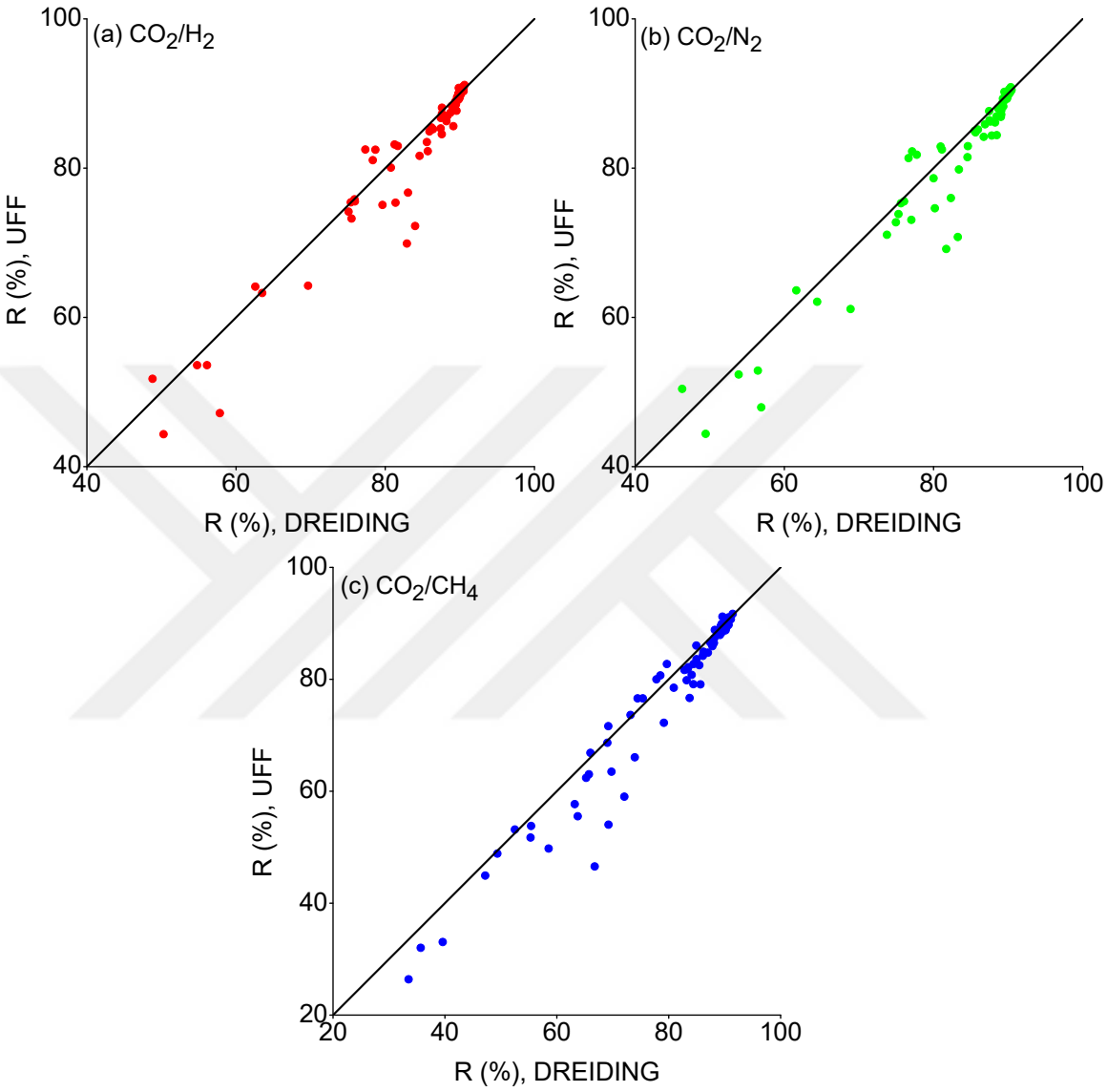

Figure 4.5. Comparison of per cent regenerabilities of MOFs computed using Dreiding and UFF for (a) CO_2/H_2, (b) CO_2/N_2, (c) CO_2/CH_4 mixtures. Diagonal lines are to guide the eye.

The FFF consists of energy parameters since adsorption mainly depends on the energetic interactions, the type and the number of atoms of the MOFs:

$$FFF=\frac{\left|\sum_i^N n_i\times\frac{n_i}{N}\times\varepsilon_{i,\ DREIDING}/k_B-\sum_i^N n_i\times\frac{n_i}{N}\times\varepsilon_{i,\ UFF}/k_B\right|}{\sum_i^N n_i\times\frac{n_i}{N}\times\varepsilon_{i,\ DREIDING}/k_B} \quad (13)$$

Here, n_i is the number of atoms i, N is the total number of atoms of MOF, and ε_i/k_B is the energy parameter of the atom i. This term expresses how much the potential parameter changes when the UFF was used instead of the Dreiding. The relation between the FFF and the changes in the predicted CO_2 uptakes of MOFs was examined. The latter was defined as follows where the CO_2 uptake predicted by the Dreiding was taken as the reference:

$$\Delta N_{CO_2}\%=\left|N_{CO_2,\ DREIDING}-N_{CO_2,\ UFF}\right|/N_{CO_2,\ DREIDING}\times100 \quad (14)$$

Figure 4.6 shows the $\Delta N_{CO_2}\%$ as a function of the FFF for the MOFs. Black points in each figure represent the MOFs for which the predicted CO_2 uptakes by two different FF vary less than 35%. In fact, 24 MOFs have less than 25% change in their CO_2 uptakes for CO_2/H_2, CO_2/N_2, and CO_2/CH_4 mixtures. The FFF of MOFs shown with black points in Figure 4.6 are less than 0.1, and their average FFF is 0.05. These are the MOFs that are not sensitive to the FF type. In other words, the area at the left of the vertical dashed lines shown in Figure 4.6 shows the safe zone to the simulators, where predictions for the CO_2 uptake of MOFs would not significantly change depending on the FF used in molecular simulations. For example, EMIHAK has the lowest FFF, 0.003. Due to its low FFF, the $\Delta N_{CO_2}\%$ values for this MOF are low: 5, 7 and 3% for CO_2/H_2, CO_2/N_2, and CO_2/CH_4 mixtures, respectively. The CO_2/H_2, CO_2/N_2, and CO_2/CH_4 selectivities of EMIHAK predicted from Dreiding are 704.52, 55.12, and 16.23, respectively, and these are very

similar to the ones predicted by UFF, 636.46, 50.15, and 16.72. On the basis of the working capacity rankings, EMIHAK is the first MOF in the Dreiding list and second MOF in the UFF list for CO_2/H_2 and CO_2/N_2 mixtures and is the fifth MOF in the Dreiding list and seventh MOF in the UFF list for CO_2/CH_4. This result shows that ranking of the MOFs having low FFF is not significantly affected from the FF.

Figure 4.6 shows that if the FFF is computed to be higher than 0.1, then Dreiding and UFF are expected to make different predictions for the CO_2 uptakes of MOFs, which also means that ranking of MOF adsorbents for CO_2 separations may be different.

Red points in Figure 4.6 represent the MOFs for which the two FFs make different estimates for the CO_2 uptake. Most MOFs have more than 40% change in the CO_2 uptakes and their average FFF is 0.203. For example, LUXDEO has a high FFF, 0.42, leading to very high ΔN_{CO_2}% values of 92, 85, and 72% for CO_2/H_2, CO_2/N_2, and CO_2/CH_4 mixtures, respectively. As a result, its performance evaluation metrics significantly change depending on the FF. For example, CO_2/H_2 selectivity of LUXDEO was predicted to be 695 by the Dreiding and 1492 by the UFF. LUXDEO was in the highly selective MOF lists determined by the UFF but it did not appear in the Dreiding list. At that point, it is important to note that not all the MOFs having FFF > 0.1 have high ΔN_{CO_2}% as can be seen from Figure 4.6. There are several MOFs with FFF of 0.1−0.25, and half of them have low ΔN_{CO_2}. However, MOFs with FFFs >0.3 are the ones that show the highest deviations between Dreiding and UFF predictions for the CO_2 uptake. Therefore, it is better to use the FFF to quantitatively define the safe region: if the FFF is less than 0.1, then either the Dreiding or the UFF can be used to evaluate the CO_2 uptake and adsorption-based CO_2 separation potential of MOFs. It is also a good practice to examine why low (high) FFF leads to small (large) changes in the CO_2 uptakes. The FFF to show the change in the potential parameters of atoms was defined. For example, OWITIY has the second lowest FFF, 0.01.

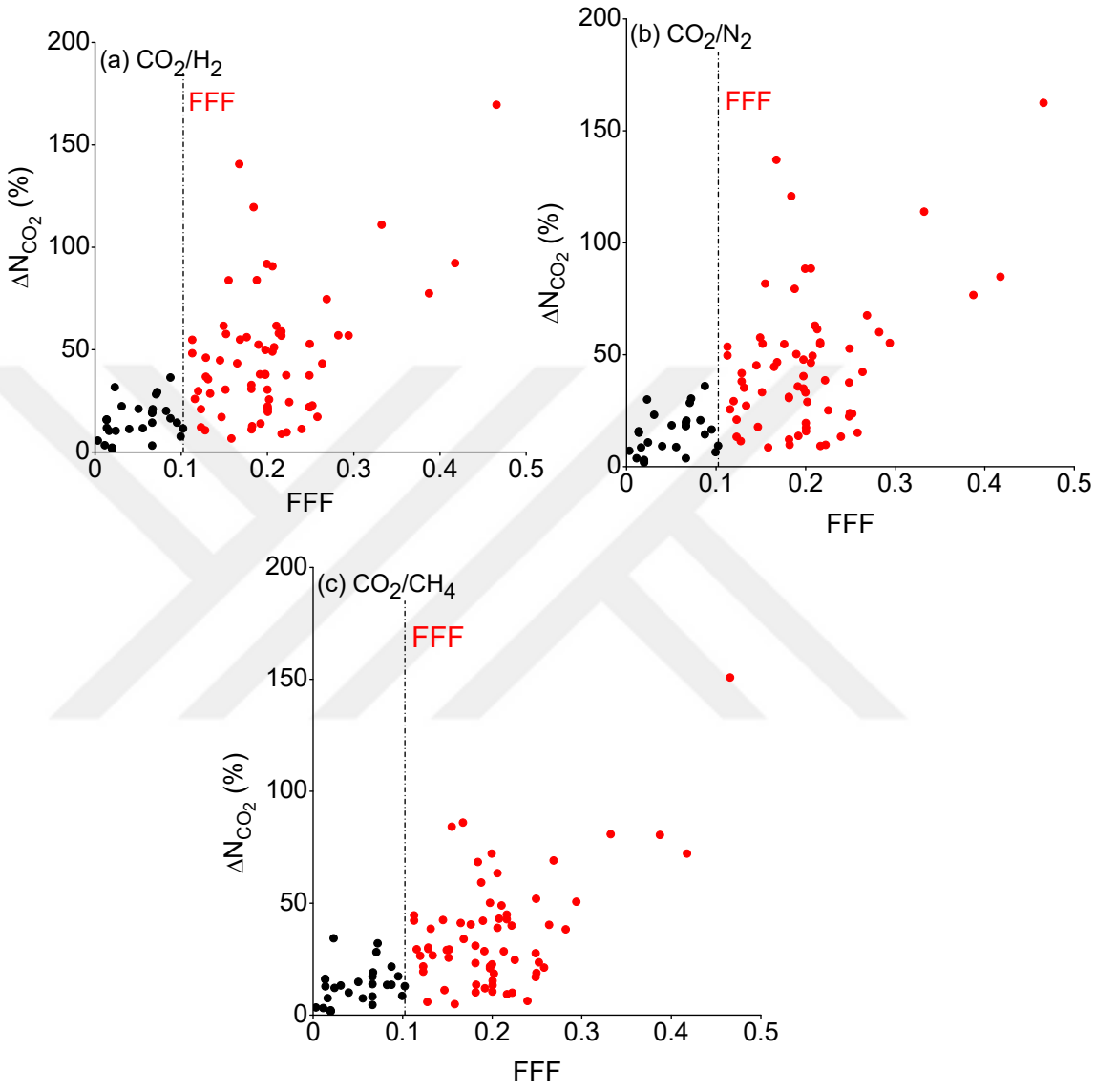

Figure 4.6. Relation between change in the CO_2 uptake and FFF for (a) CO_2/H_2, (b) CO_2/N_2, (c) CO_2/CH_4 mixtures. The vertical dashed lines are given to differentiate between the MOFs that are sensitive to the FF type (on the right) and the ones that are not sensitive to the FF type (on the left).

This MOF has Mn, and since its energy parameter is not available in Dreiding, it was taken from the UFF. Therefore, there is no difference for the ε/k_B of metal atoms.

The energy parameters of 144 C and 52 H atoms increased from 47.88 to 52.87 K and 7.65 to 22.15 K, respectively, when the UFF was used instead of the Dreiding. However, this increase was balanced by the decrease in the energy parameters of 96 O atoms from 48.19 to 30.21 K. As a result, the FFF is small for that MOF. In other words, the increase in the energy parameters of (C + H) is balanced with the decrease in energy parameters of (N + O) for the MOFs having low FFFs. In contrast, MOFs with high FFFs are either those having a metal atom which shows a large change when the FF is switched from Dreiding to UFF (such as OFERUN) or those having a large number of C and H atoms in their structures (such as GUPCOK). In the case of OFERUN, the energy parameter of Zn significantly increases when the UFF was used and leads to a high FFF of 0.39. GUPCOK has large number of C and H atoms, and the UFF part of the Eq 1 dominates the Dreiding part and leads to a large FFF of 0.46 for that MOF. Supporting this argument, the average of ratio of sum of C and H atoms to the total number of atoms in MOFs is 0.76 for the MOFs having high FFF whereas it is 0.62 for the MOFs having low FFFs. Atoms type and numbers of the MOFs having the five lowest and highest FFFs are also given in Table B4.

Finally, it is important to note that the aim is to arbitrarily define a simple parameter that can be very quickly calculated before the molecular simulations to make a decision of using either Dreiding or UFF. Several other factors which affect the adsorption strength of the gases in the MOFs such as topology of the material, pore size, and pore shape have not been considered in the definition of FFF. The usefulness of the FFF is the following: Before computationally demanding simulations, one can calculate the FFF within seconds only considering the number and type of the atoms present in the MOF. If this value is smaller than 0.1, then either of the generic FFs can be used, since they will give similar estimates for CO_2 uptakes of MOFs and hence similar rankings of the MOF adsorbents.

However, having a low FFF does not mean that either Dreiding or UFF are necessarily accurate for this MOF, it just means that they are interchangeable. There may be cases that the best thing to do would be to use neither and develop a new model. If the FFF is higher than 0.1, significant quantitative differences can be expected for the CO_2 predictions of the Dreiding and UFF. In this case, obtaining experimental data to validate the selection of the FF or performing more detailed quantum-level calculations can be considered since the MOF is sensitive to the FF type.

Chapter 5

Computational Screening of MOFs for H_2S Separation from $H_2S/CH_4/CO_2$ Mixture

In Chapter 4, we explored the ranking of the materials for CO_2 separation from binary mixtures. However, mixtures are most likely not binary but multi-component in the industrial applications, such as natural gas, fuel gas or landfill gas. Therefore, it is important to distinguish how adsorbent evaluation metrics would change when multi-component mixtures are studied. While CH_4 is the main component of natural gas, biogas, landfill gas or fuel gas, there are also undesirable components in these gas mixtures such as H_2S and/or CO_2. For example, the mixture including these components is called sour natural gas and acidic component causes corrosion at storage or transportation of the desired gas. Further, SO_2 releases from combustion of gas mixture including H_2S such as refinery fuel gas. SO_2 release causes to acid rain with combining water vapor in the air. This formation has critical impact on both the environment and human health. Motivated from this, we studied on H_2S separation from H_2S/CH_4 binary mixture and then $H_2S/CH_4/CO_2$ ternary mixture as considering fuel gas.

GCMC simulation was performed using RASPA open code for 4213 MOFs.[109] These simulations were performed 303 K and adsorption pressure of 1bar and desorption pressure of 4 bar. GCMC simulations were performed for binary H_2S/CH_4 mixture and ternary mixture of $H_2S/CH_4/CO_2$. Compositions of mixtures were set to 1:99 and 0.2:29.8:70, respectively. Four different moves were considered for GCMC simulations including translation, reinsertion, swap and identity exchange of a molecule. The Lorentz−Berthelot mixing rules were employed. The cutoff distance for truncation of the intermolecular interactions was set to 13 Å. Periodic boundary conditions were applied in

all simulations. Simulations were executed for 1000 cycles with the first 5000 cycles for initialization and the last 5000 cycles for taking ensemble averages. Lennard-Jones 12-6 potential was used to model CO_2[99] and CH_4[102] as presented in previous part of the thesis. H_2S molecules were modeled using LJ 12-6 potentials as four-site rigid molecules. Two sites are located at the H atoms and one site is located at the S atoms, fourth site is located at the center of the mass with partial point charges.[110] LJ 12-6 potential from UFF is used for the MOFs. All performance metrics were computed for the GCMC results as presented in Chapter 3.

We first compared our results with the experimentally reported results of single-component H_2S uptake in MOFs, MIL-47(V), MIL-53(Cr), MIL-53(Al), MIL-100(Cr), and MIL-101(Cr).[111] We obtained a good agreement between our simulations and experiment in terms of H_2S uptake for those materials as shown in Figure 5.1.a. We also computed the summation of H_2S and CO_2 adsorption for ternary mixture of $H_2S/CH_4/CO_2$ and compared with an available simulation study under the same conditions[112] and showed the good agreement with the previously reported results in Figure 5.1.b. With this motivation, we studied 4213 MOFs to investigate their H_2S separation performances.

We first examined the binary H_2S/CH_4 mixture, and then proceeded with ternary mixture of $H_2S/CH_4/CO_2$. Figure 5.2 shows H_2S/CH_4 selectivity and H_2S working capacity of MOFs predicted at an adsorption pressure of 4 bar and desorption pressure of 1 bar. The selectivity ranges from 1.6 to 4890 as shown in Figure 5.2. In the literature, most of the studies presented that H_2S/CH_4 selectivity is generally lower than 100. For example, H_2S/CH_4 selectivity of UiO-66 (Zr),[113] MIL-47,[114] MIL-125 (Ti),[115] zeolites,[116] HKUST-1,[117] and UiO-66 (67,68)[118] was reported to be lower than 100 at different studies. Bobbitt et al.[119] and Li et al.[120] reported that H_2S/CH_4 selectivity of Cu-TDPAT at 298 K is in the range of 100-200.

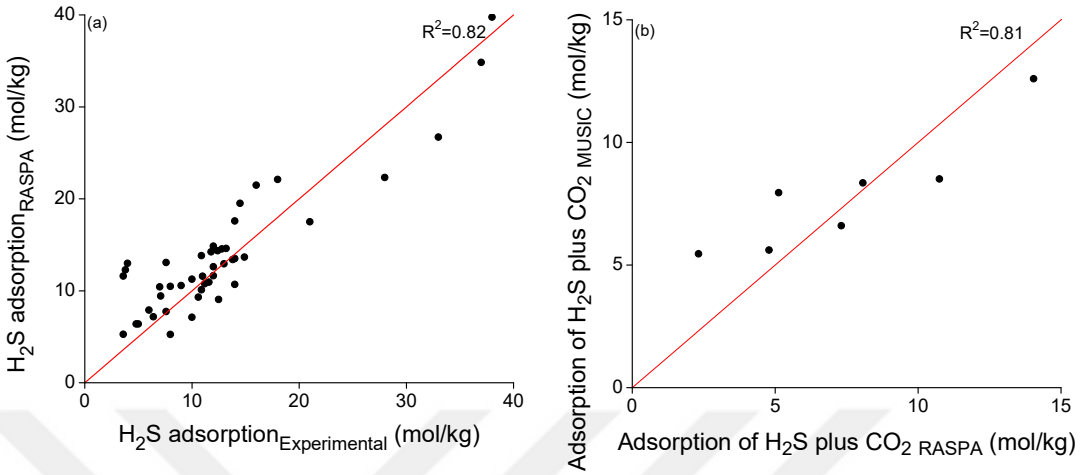

Figure 5.1. (a) Comparison of our simulation results and experimental data for single-component H_2S uptake (b) Comparison of our simulation results and different simulation results for H_2S plus CO_2 uptake in of $H_2S/CH_4/CO_2$ ternary mixture.

Ninety percent of MOFs examined in this work has a selectivity lower than 200, however there are also highly selective (>1000) MOFs among our materials as suggested by Li[121] and Hong.[122]. They explored the H_2S/CH_4 selectivity of the functionalized UiO-66(Zr) and ZIF-80 and presented the selectivity in the range of 100-1000 and 200-1300, respectively.

H_2S working capacity varies from 0.0000196 to 3 mol/kg at an adsorption pressure of 4 bar and desorption pressure of 1 Bar. We can see that most of the highly selective materials (>1000) have low working capacity (<0.1 mol/kg). We expect that promising materials should have high selectivity and high working capacity. Thus, the multiplication of these parameters (APS) is very convenient to identify the best material candidates. We classified materials into four regions based on their APS values (APS =100, APS =500, and APS=1500) to determine the materials with low and high performance. The APS values of 3802 and 95 MOFs from 4213 materials are lower than 100 and higher than 500, respectively. It is important to distinguish the materials, which have very high selectivity

(>500) or working capacity (>2.5 mol/kg), although their corresponding selectivity or working capacity are very low as shown in Figure 5.2.

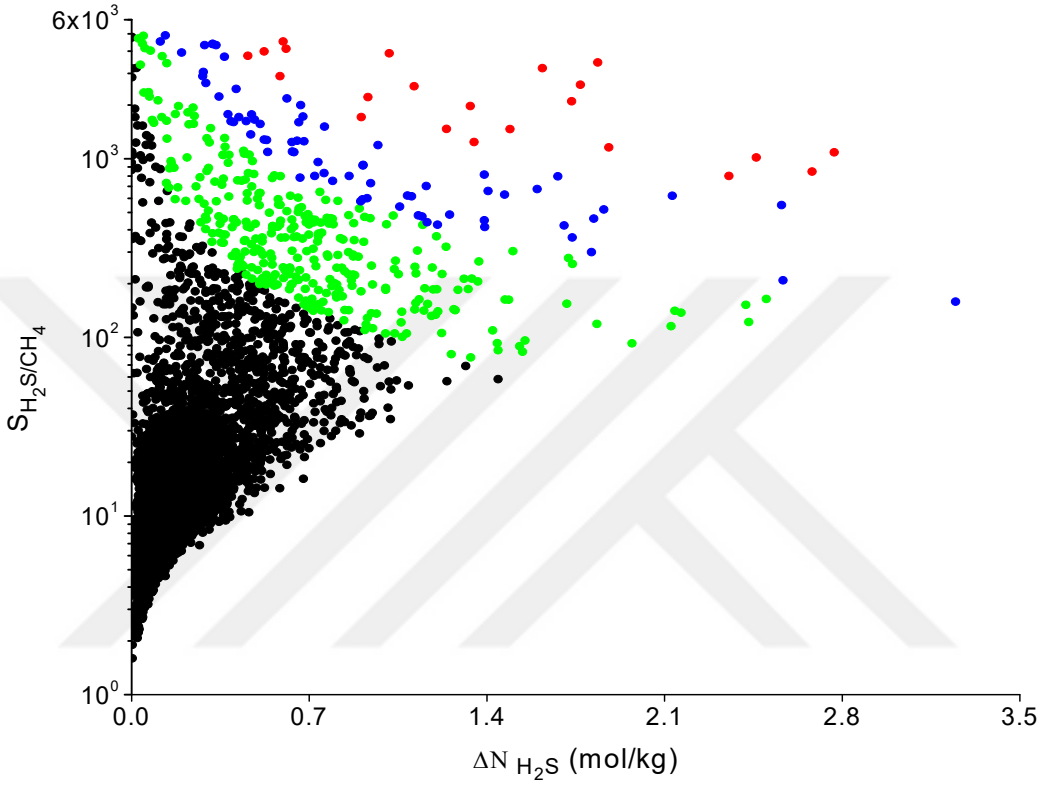

Figure 5.2. Relation between selectivity (S), working capacity (ΔN) and adsorbent performance score (APS) of 4213 MOFs for calculated at adsorption pressure of 4 bar.

For example, materials with high selectivity (>500) usually exhibit low working capacity (0.2 kg/mol), and materials with high working capacity (>1.2 kg/mol) usually exhibit low selectivity (<50) as seen in the black region of Figure 5.2. The black region also represents a large number of 4213MOFs which have moderate selectivity (20-500) and working capacity (0.6-1.4 kg/mol). MOFs with APS in the range between 100 and 500 are a group of promising materials shown in the green region of Figure 5.2.

The blue and red regions of the same figure represent the most promising MOFs with high APS values (>500). Selectivities (working capacities) of MOFs in these regions range from 158 to 4890 (0.11-3.25). We determined 22 MOFs from 4213 with high APS values (>1500) as the top performing structure in the red region. They represent the most desired combination of selectivity (in the range of 800-4529) and working capacity (in the range of 0.46-2.72 mol/kg). For example, FAGZAO has the highest APS value (6347 mol/kg) and its corresponding selectivity and working capacity values are 3455 and 1.84 kg/mol, respectively. Other promising materials in the red region are LAKHOV, DATKIU, PEVVAO, and CUSDIE. They present both high selectivity of 1085, 847, 1013, 800, and high working capacity of 2.77, 2.68, 2.46, 2.35, respectively. However, some materials have the same trade-off between selectivity and working capacity in the red region. MOFs with very high selectivity (>2000) have low working capacity (<0.6 kg/mol) as shown in Figure 5.2.

Other important metrics to evaluate the performance of the materials are S_{sp} and regenerability (%). S_{sp} values of MOFs changes between 0.02 and 0.7×10^6 while most of MOFs (3256 from 4226) are located in the same region where S_{sp} is 1-4000 as shown in Figure 5.3. The selectivity of these MOFs varies from 1 to 1000. XAFXOT, CUCFUD and SUGVUM are the most promising materials, which are displayed at the right corner of Figure 5.3 with red color. They have both high selectivity and S_{sp} with the values of 4412, 4529, 4797 and 0.4×10^6, 0.2×10^6, and 0.1×10^6, respectively.

We presented the relation between regenerability (R%) and selectivity plus APS of 4213 MOFs in Figure 5.4. They exhibit very wide range in terms of R (%) from 0.015 to 82.3%. However, it is important to note that regenerability of MOFs is quite low because only 198 MOFs from 4213 have R%>75%. Although PIHJOH03 is the most promising material in terms of R% (82%), it has very low selectivity (4.9) as seen in Figure 5.4.a. Moreover, some MOFs have higher selectivity (>1000) but they suffer from low R% (<20%). In Figure 5.4.a, we color-coded the promising materials as red. R% of ENISUQ

and KITGUQ are very high (78% and 79%) with also high selectivities (358 and 162). We plotted R% also as a function of APS and we marked promising MOFs above the red line and the ones with the highest APS value in Figure 5.4.b. KITGUQ was still promising material while ENISUQ was not determined as promising because of its low APS and accordingly working capacity value.

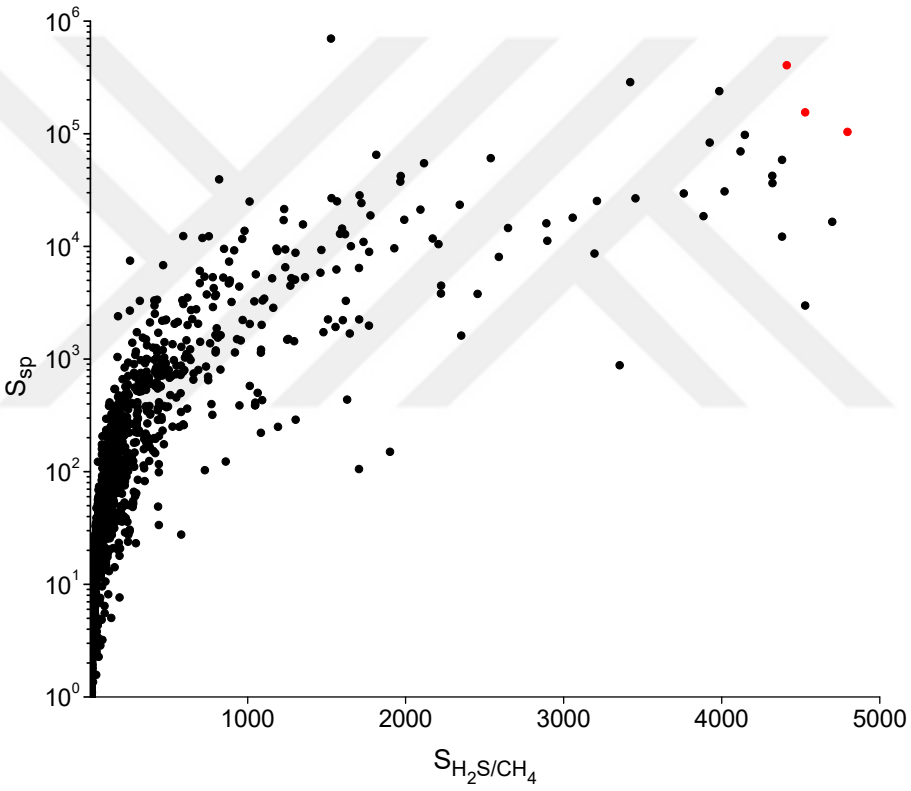

Figure 5.3. Sorbent selection parameters and selectivities of MOFs. Red dots represent promising materials.

We can conclude that selectivity is not an adequate parameter to evaluate the most promising materials. Regenerability has a strong influence to decide the promising MOFs for gas separation. Therefore, we extended our search by the strategy of the determination

of the MOFs with R>%75. Among these, we chose the top 20 materials based on APS and selectivity and compared the results. Fifteen of MOFs, which are ACOQEP, AHOZII, BODYID, CAYSIE, ENISUQ, FIZQAI, HUYKER, ILIGOZ, KITGUQ, ODIPAS, OHOFIA, REQBOG, VEQBID, XESKAJ, and XUMMUP, are common in Table 5.1 and Table 5.2 and presented in bold as shown in both two tables. KITGUQ, ACOQEP, ODIPAS, and ILIGOZ are the best adsorbent in terms of all performance metrics among 4213 MOFs and they are located at almost the same places in both of two lists.

Once we identified the best MOF with binary mixture of H_2S/CH_4, we proceeded our study with computing adsorption of ternary mixture of $H_2S/CH_4/CO_2$ in these top 20 MOFs Ternary mixture results in terms of APS, selectivity and working capacity were compared with those computed for binary mixture. H_2S selectivities predicted for ternary mixture are generally higher than the ones predicted for binary mixture, while the selectivity for binary and ternary mixture is not highly different. However, H_2S working capacity is quite different for binary and ternary mixture, and working capacities calculated for ternary mixtures are lower than the ones of binary mixtures. Therefore, APS values for ternary mixture are also quite lower than the ones for binary mixtures. Even though numeric values of metrics are different, the ranking of the MOFs based on selectivity computed for binary mixture is highly similar to the ranking computed for ternary mixtures. For example, first, sixth, seventh and last four materials are same for both binary and ternary mixture simulations. Seven of top ten MOFs is same with similar ranking based on binary and ternary simulation results. The SRCC between selectivity for binary and ternary mixtures is calculated as 0.82. It is concluded that molecular simulations conducted for H_2S separation from binary mixtures are also useful to determine the promising materials for the ternary mixtures.

Investigation on a large number of materials with various structural and topological properties is a very good opportunity to examine the structure-performance

relationship. This investigation might provide the synthesis of new MOFs with better performances and also helps to determine the promising MOFs among thousands.

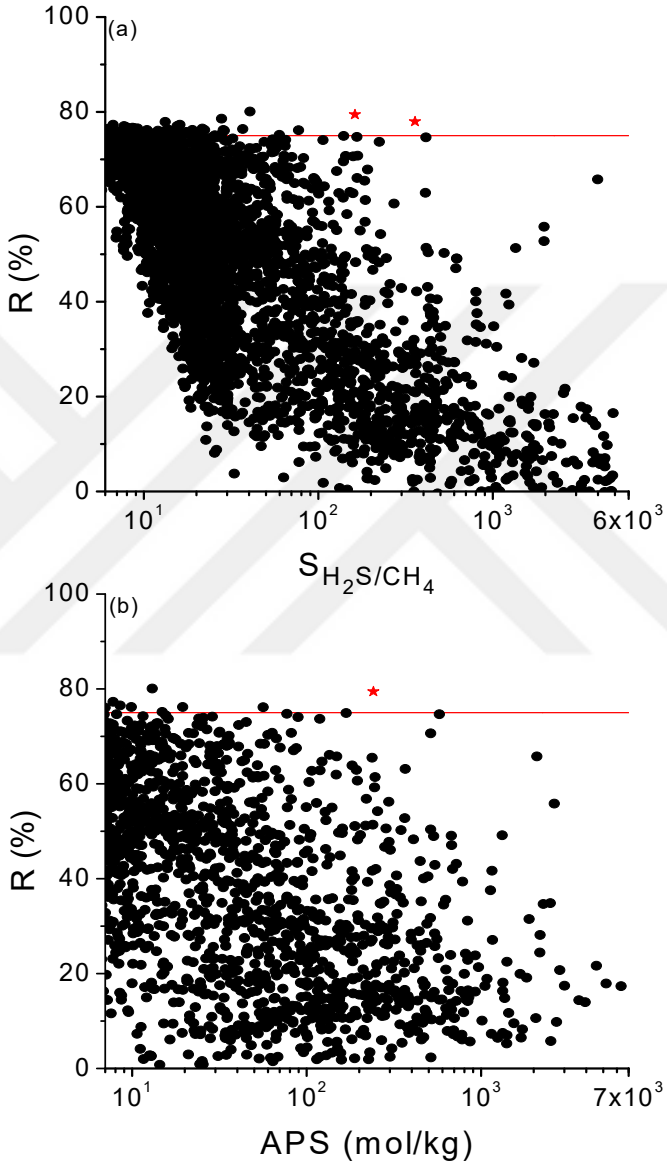

Figure 5.4. Relation between R % and (a) selectivity and (b) APS. Red solid lines represent R% =75 and red stars indicate promising MOFs.

Table 5.1. Ranking of Top 20 MOFs Depending on Selectivity

MOFs	$S_{H2S/CH4}$	ΔN H_2S (mol/kg)	R (%)	APS (mol/kg)
ENISUQ	358.04	0.01	77.97	3.90
KITGUQ	162.13	1.49	79.46	241.05
ACOQEP	76.92	0.73	76.09	56.35
ODIPAS	59.75	0.25	75.15	14.85
ILIGOZ	40.58	0.32	80.05	13.04
OGUTOA	36.92	0.01	76.39	0.19
VEQBID	28.95	0.24	76.02	7.00
AHOZII	28.57	0.68	76.14	19.44
OHOFIA	27.98	0.23	75.37	6.52
IQOYET	27.86	0.00	78.57	0.00
PYNICL01	25.47	0.09	75.03	2.28
BODYID	22.31	0.44	76.14	9.87
XESKAJ	21.63	0.39	76.48	8.52
HUYKER	20.98	0.26	75.90	5.56
YEMMAF	19.09	0.07	75.06	1.42
REQBOG	18.95	0.13	76.22	2.45
PITYUN01	17.46	0.05	75.75	0.84
FIZQAI	16.11	0.48	77.26	7.77
XUMMUP	15.89	0.20	77.11	3.23
CAYSIE	15.53	0.17	77.00	2.68

Table 5.2. Ranking of Top 20 MOFs Depending on APS

MOFs	$S_{H2S/CH4}$	ΔN H_2S (mol/kg)	R (%)	APS (mol/kg)
KITGUQ	162.13	1.49	79.46	241.05
ACOQEP	76.92	0.73	76.09	56.35
AHOZII	28.57	0.68	76.14	19.44
ODIPAS	59.75	0.25	75.15	14.85
ILIGOZ	40.58	0.32	80.05	13.04
BODYID	22.31	0.44	76.14	9.87
XESKAJ	21.63	0.39	76.48	8.52
FIZQAI	16.11	0.48	77.26	7.77
VEQBID	28.95	0.24	76.02	7.00
OHOFIA	27.98	0.23	75.37	6.52
HUYKER	20.98	0.26	75.90	5.56
ENISUQ	358.04	0.01	77.97	3.90
FEHCOM	12.01	0.31	75.15	3.67
FIRNAX	10.98	0.31	75.31	3.45
XUMMUP	15.89	0.20	77.11	3.23
LONVIV	14.77	0.21	75.96	3.16
KOCWEF	11.05	0.25	75.18	2.71
CAYSIE	15.53	0.17	77.00	2.68
FIRNAX01	9.63	0.28	75.32	2.65
REQBOG	18.95	0.13	76.22	2.45

We examined the correlation between selectivities of MOFs at adsorption and desorption pressure and their structural properties, such as pore sizes, porosities and surface areas. In Figure 5.5, the relation between selectivity and LCD of MOFs is

presented. It displays that selectivity increases with decrease in the LCD since gas molecules favor the small cavities due to their strong confinements. However, the inverse relationship is not valid for some MOFs. For example, some MOFs with LCD between 15-20 Å have also high selectivity (200-1000). Even this relation is not perfectly fit to all MOFs, some MOFs whose LCD is lower than 15 Å offer lower (<20) selectivity.

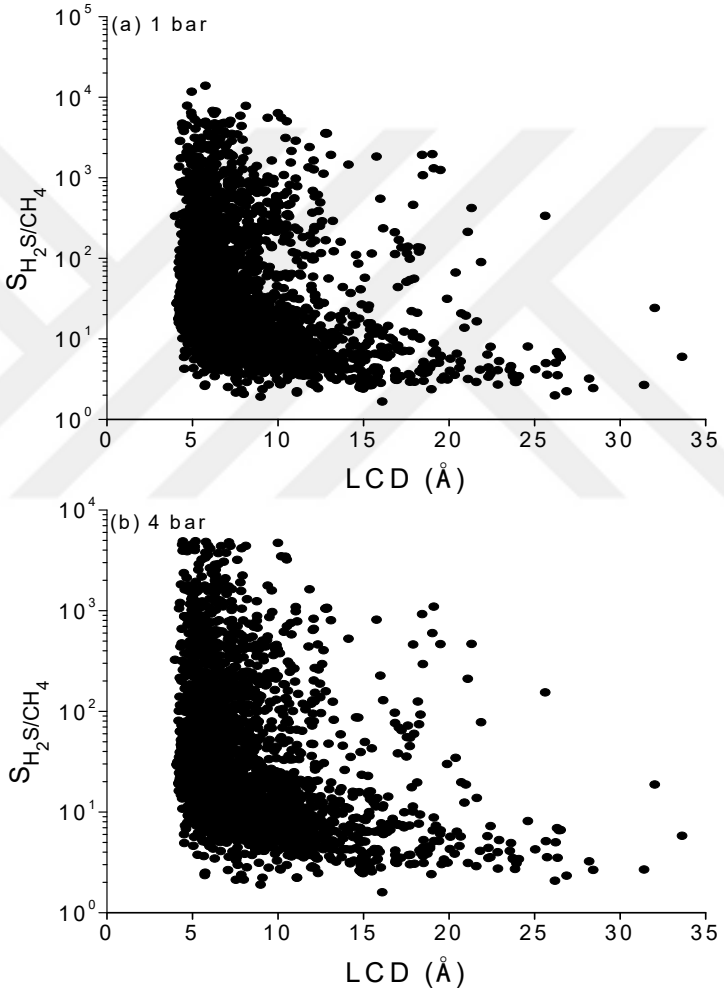

Figure 5.5. Relation between the LCDs and selectivities of 4213 MOF at (a) 1 bar (b) 4 bar.

Figure 5.6 shows that as volume fraction (porosity) of MOFs increases, the selectivities decrease since all components of mixture are easily adsorbed in MOF. Hence, MOFs with high volume fraction exhibit low selectivity.

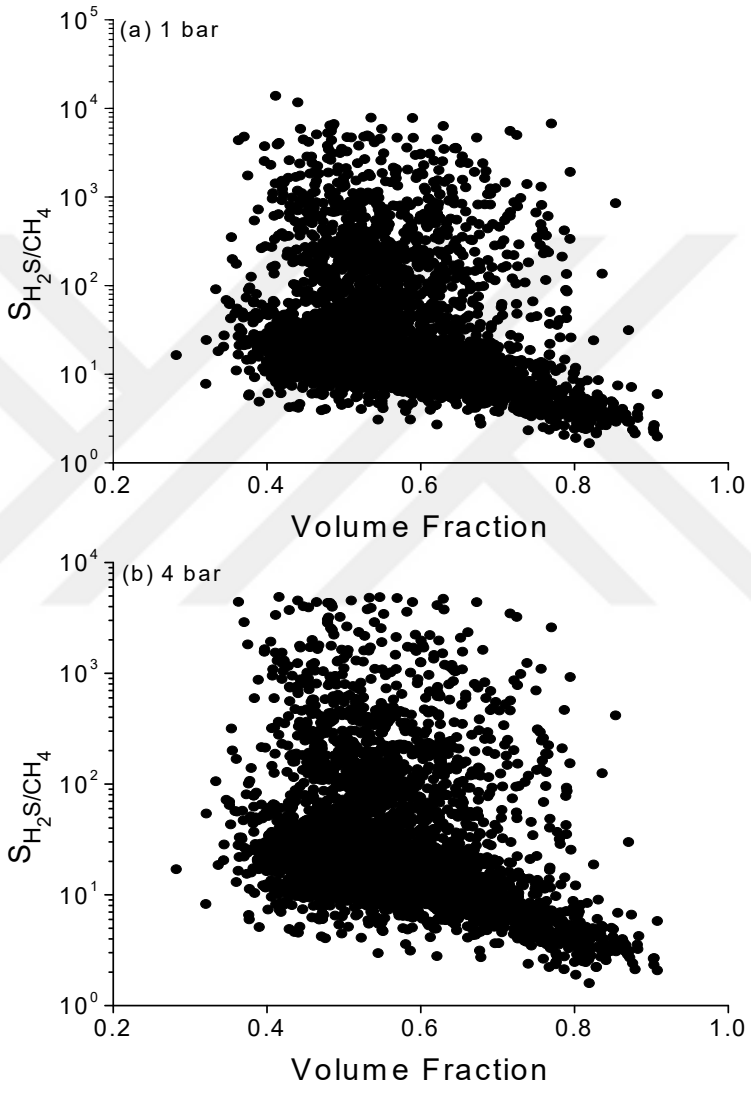

Figure 5.6. Relation between the volume fractions and selectivities of 4213 MOF at (a) 1 bar (b) 4 bar.

In Figure 5.7, the relation between selectivity and surface areas of MOFs is shown. Although this relation is not strongly adequate, the selectivity decreases with the increasing surface areas of materials for most of MOFs. For example, almost all MOFs with high surface area (>4000 m^2/g) have low selectivity (<10).

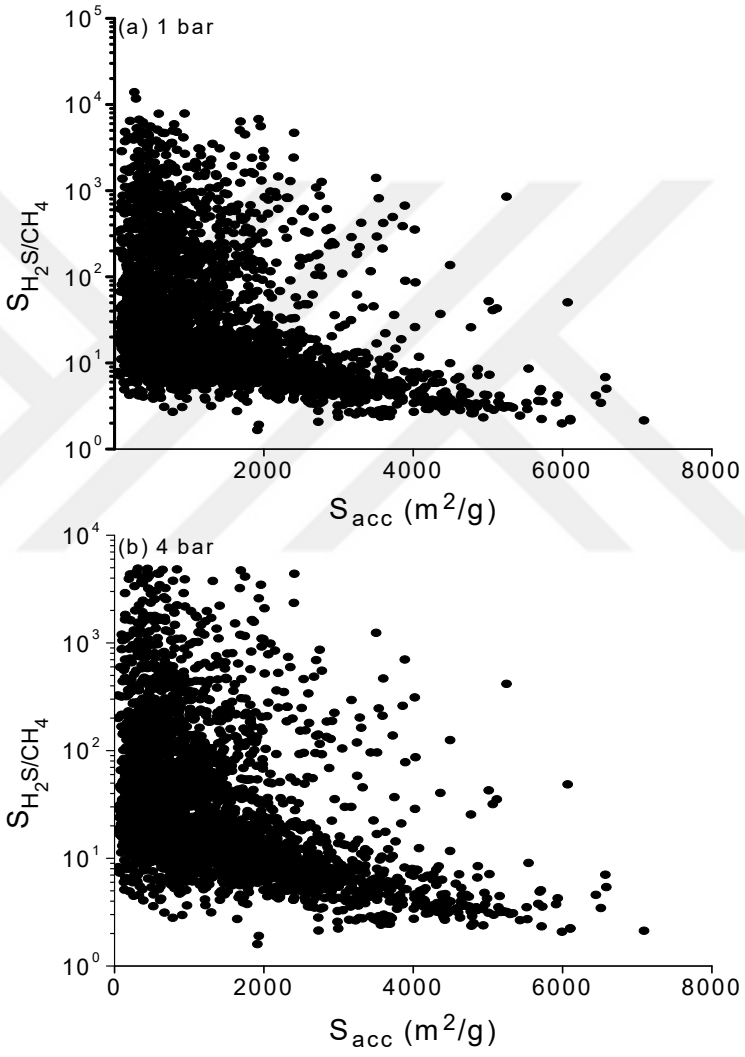

Figure 5.7. Relation between the accessible surface areas and selectivities of 4213 MOF at (a) 1 bar (b) 4 bar.

We also investigated the structural properties of top 20 materials based on selectivity and APS as displayed in Figure 5.8.a and Figure 5.8.b, respectively. Outer circles and inner circles display 4213 MOFs and top 20 most selective (top 20 APS) based on the corresponding structural properties, respectively. Results indicated that the MOFs with 3.8Å<PLD<5 Å, 5Å<LCD<7.5Å, 0.5<ϕ< 0.75, 1 g/cm^3<ρ<1.5g/cm^3 and SA<1000 m^2/g (1000 m^2/g<SA<2000 m^2/g for top 20 in terms of APS) are the promising materials with respect to both selectivity and APS. When it is considered that there is a trade-off between selectivity and working capacity, it is important to determine the MOFs with both high selectivity and APS (multiplication of selectivity and working capacity). Since the 15 materials from top 20 MOFs can be considered identical based on selectivity and APS data, structural criteria belonging to these MOFs in terms of selectivity and APS are also same. Therefore, these criteria and materials are very precious for H_2S separation.

(a)

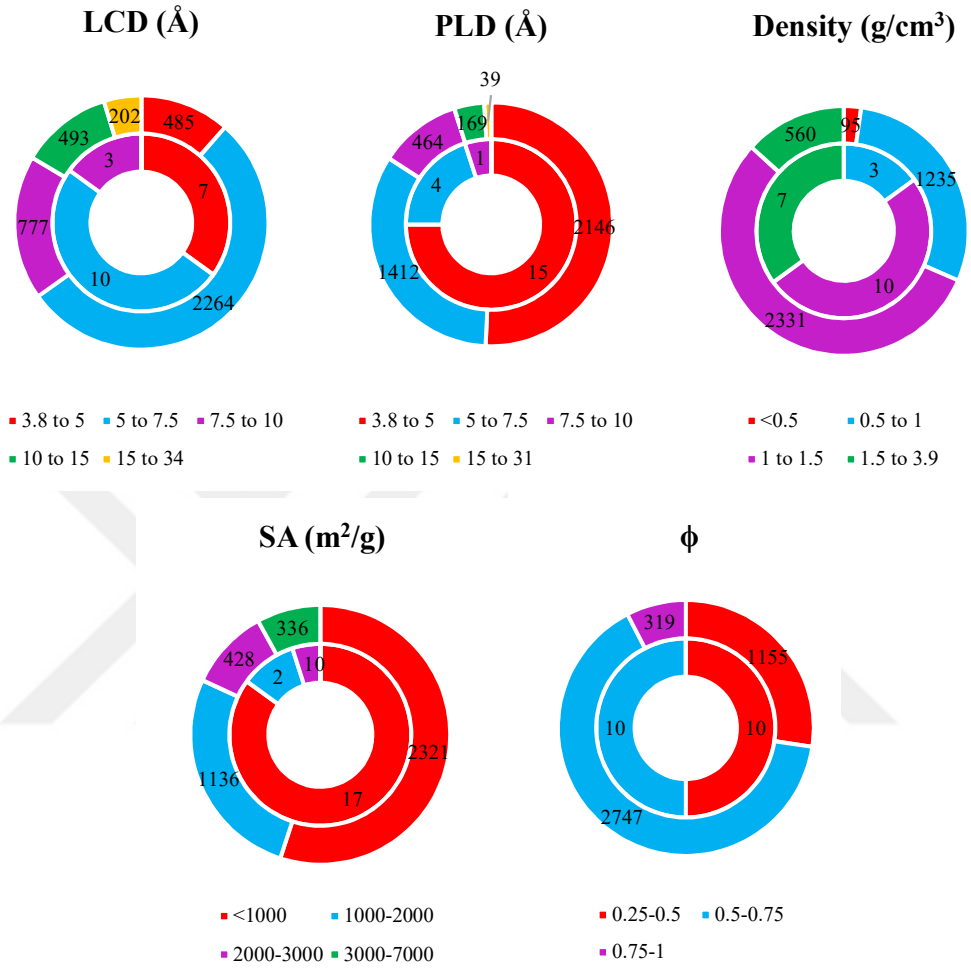
LCD (Å)
485
7
2264
10
777
3
493
202
3.8 to 5
5 to 7.5
7.5 to 10
10 to 15
15 to 34
PLD (Å)
39
169
464
1
4
2146
1412
15
3.8 to 5
5 to 7.5
7.5 to 10
10 to 15
15 to 31
Density (g/cm3)
95
3
1235
7
10
2331
560
<0.5
0.5 to 1
1 to 1.5
1.5 to 3.9
SA (m2/g)
336
428
2
10
2321
1136
17
<1000
1000-2000
2000-3000
3000-7000
ϕ
319
1155
10
10
2747
0.25-0.5
0.5-0.75
0.75-1

(b)

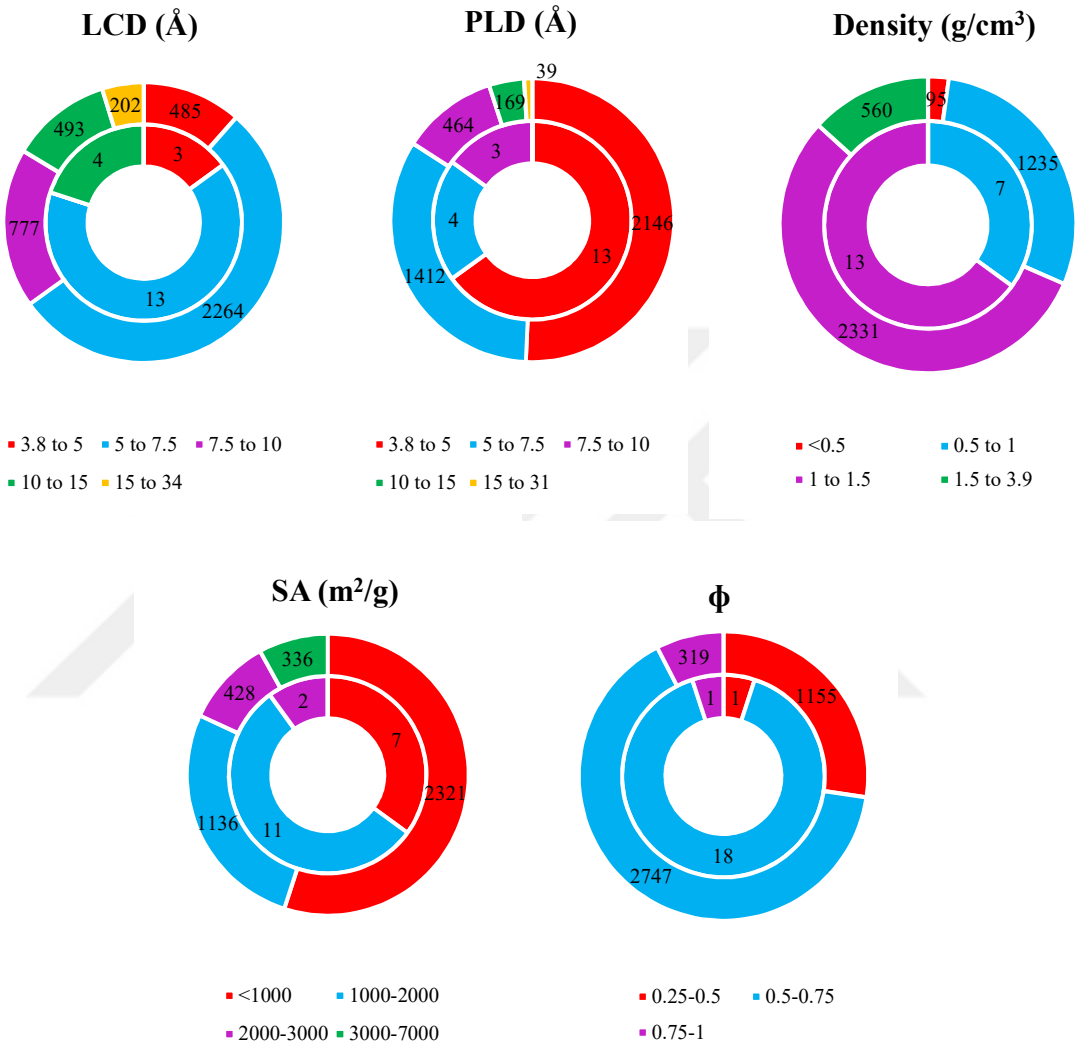

Figure 5.8. Impact of structural properties on the H_2S separation performances of MOFs. Outer circle shows the 4213 MOFs and inner circle shows top 20 performing MOFs in terms of (a) selectivity (b) APS.

Chapter 6

Conclusions

The impact of the FF selection on high throughput computational screening of MOFs for CO_2/H_2, CO_2/N_2, and CO_2/CH_4 separations was investigated. Molecular simulations using Grand Canonical Monte Carlo techniques based on Dreiding for 100 MOFs were performed and these simulations were repeated using UFF to compute adsorption of CO_2/H_2, CO_2/N_2, and CO_2/CH_4 mixtures. Four adsorbent evaluation metrics, which are selectivity, working capacity, sorbent selection parameter, and regenerability, were calculated using the results of Dreiding- and UFF-based simulations and they were compared. Results showed that while there are quantitative differences in the computed metrics, ranking of MOFs is similar for two different FFs, especially in terms of selectivity and regenerability, which are the key parameters to select the most promising materials. Therefore, it is concluded that both FFs can be used in high-throughput molecular simulations of MOFs to identify the useful materials for adsorption-based CO_2 separations. A FFF was also defined and its relation with the change in CO_2 uptakes of MOFs was showed to guide the simulators. If the FFF value of a MOF is lower than 0.1, then the role of the FF on the CO_2 uptake predictions is negligible; however, if the FFF is higher than 0.3, then significant quantitative differences in the predicted CO_2 uptakes, adsorbent evaluation metrics, and MOF rankings can be observed. With this FFF, the safe region in which the results of molecular simulation do not significantly change depending on the type of generic FF is shown. These results will be of great interest for researchers working on molecular simulations of MOFs by providing insights into choosing the appropriate FF. In addition, a screening of 4213 MOFs from Cambridge Structural

Database was performed to determine the high-potential materials for use to separate H_2S from H_2S/CH_4 mixture. We computed all performance criteria for the entire material database. The strategy to determine the top performing MOFs was as follows: APS values for H_2S/CH_4 mixture were used to rank highly regenerable MOFs. In order to achieve a more useful evaluation for the real industrial applications, we investigated the top performing materials using GCMC simulation for ternary mixture of $H_2S/CH_4/CO_2$. The relationship between structure and performance was enlightened for the designing a new, high-potential MOF for the separation of H_2S. We observed that the MOFs with the following values are the promising materials in terms of selectivity and APS: 3.8Å<PLD<5 Å, 5Å<LCD<7.5Å, 0.5<ϕ<0.75, 1 g/cm^3<ρ<1.5g/cm^3 and SA<1000 m^2/g (1000 m^2/g<SA< 2000 m^2/g for top 20 in terms of APS).

BIBLIOGRAPHY

1. Root, T. L.; Price, J. T.; Hall, K. R.; Schneider, S. H.; Rosenzweig, C.; Pounds, J. A., Fingerprints of global warming on wild animals and plants. *Nature* **2003,** *421* (6918), 57-60.
2. Mondal, M. K.; Balsora, H. K.; Varshney, P., Progress and trends in CO2 capture/separation technologies: A review. *Energy* **2012,** *46* (1), 431-441.
3. Meisen, A.; Shuai, X. S., Research and development issues in CO2 capture. *Energ Convers Manage* **1997,** *38*, S37-S42.
4. Aaron, D.; Tsouris, C., Separation of CO2from Flue Gas: A Review. *Separation Science and Technology* **2005,** *40* (1-3), 321-348.
5. Liu, Y.; Wang, Z. U.; Zhou, H.-C., Recent advances in carbon dioxide capture with metal-organic frameworks. *Greenhouse Gases: Science and Technology* **2012,** *2* (4), 239-259.
6. Furukawa, H.; Cordova, K. E.; O'Keeffe, M.; Yaghi, O. M., The chemistry and applications of metal-organic frameworks. *Science* **2013,** *341* (6149), 1230444.
7. Keskin, S., Recent Advances in Molecular Dynamics Simulations of Gas Diffusion in Metal Organic Frameworks. In *Molecular Dynamics-Theoretical Developments and Applications in Nanotechnology and Energy*, IntechOpen: 2012.
8. Meek, S. T.; Greathouse, J. A.; Allendorf, M. D., Metal-organic frameworks: A rapidly growing class of versatile nanoporous materials. *Advanced Materials* **2011,** *23* (2), 249-267.
9. Qiu, S.; Xue, M.; Zhu, G., Metal–organic framework membranes: from synthesis to separation application. *Chemical Society Reviews* **2014,** *43* (16), 6116-6140.
10. Belmabkhout, Y.; Guillerm, V.; Eddaoudi, M., Low concentration CO_2 capture using physical adsorbents: Are metal–organic frameworks becoming the new benchmark materials? *Chemical Engineering Journal* **2016,** *296*, 386-397.
11. Keskin, S.; van Heest, T. M.; Sholl, D. S., Can Metal–Organic Framework Materials Play a Useful Role in Large-Scale Carbon Dioxide Separations? *ChemSusChem* **2010,** *3* (8), 879-891.
12. Li, J.-R.; Ma, Y.; McCarthy, M. C.; Sculley, J.; Yu, J.; Jeong, H.-K.; Balbuena, P. B.; Zhou, H.-C., Carbon dioxide capture-related gas adsorption and separation in metal-organic frameworks. *Coordination Chemistry Reviews* **2011,** *255* (15), 1791-1823.
13. Lu, X.; Jin, D.; Wei, S.; Wang, Z.; An, C.; Guo, W., Strategies to enhance CO_2 capture and separation based on engineering absorbent materials. *Journal of Materials Chemistry A* **2015,** *3* (23), 12118-12132.
14. Ben-Mansour, R.; Habib, M.; Bamidele, O.; Basha, M.; Qasem, N.; Peedikakkal, A.; Laoui, T.; Ali, M., Carbon capture by physical adsorption: Materials, experimental

investigations and numerical modeling and simulations–A review. *Applied Energy* **2016,** *161*, 225-255.
15. Stock, N.; Biswas, S., Synthesis of metal-organic frameworks (MOFs): routes to various MOF topologies, morphologies, and composites. *Chemical reviews* **2011,** *112* (2), 933-969.
16. Colon, Y. J.; Snurr, R. Q., High-throughput computational screening of metal-organic frameworks. *Chemical Society Reviews* **2014,** *43* (16), 5735-5749.
17. Jiang, J. W.; Babarao, R.; Hu, Z. Q., Molecular simulations for energy, environmental and pharmaceutical applications of nanoporous materials: from zeolites, metal-organic frameworks to protein crystals. *Chemical Society Reviews* **2011,** *40* (7), 3599-3612.
18. Bao, Y.; Martin, R. L.; Simon, C. M.; Haranczyk, M.; Smit, B.; Deem, M. W., In silico discovery of high deliverable capacity metal–organic frameworks. *The Journal of Physical Chemistry C* **2014,** *119* (1), 186-195.
19. Thornton, A. W.; Simon, C. M.; Kim, J.; Kwon, O.; Deeg, K. S.; Konstas, K.; Pas, S. J.; Hill, M. R.; Winkler, D. A.; Haranczyk, M., Materials genome in action: identifying the performance limits of physical hydrogen storage. *Chem Mater* **2017,** *29* (7), 2844-2854.
20. Frenkel, D.; Smit, B., *Understanding Molecular Simulation: From Algorithms to Applications*. 2 ed.; Academic Press: San Diego, 2002.
21. Bordiga, S.; Vitillo, J. G.; Ricchiardi, G.; Regli, L.; Cocina, D.; Zecchina, A.; Bj.Arstad; Bjørgen, M.; Hafizovic, J.; Lillerud, K. P., Interaction of hydrogen with MOF-5. *Journal of Physical Chemistry B* **2005,** *109*, 18237-18242.
22. Sagara, T.; Klassen, J.; Ganz, E., Computational study of hydrogen binding by metal-organic framework-5. *Journal of Chemical Physics* **2004,** *121* (24), 12543-12547.
23. Tafipolsky, M.; Amirjalayer, S.; Schmid, R., Ab initio parametrized MM3 force field for the metal-organic framework MOF-5. *Journal of Computational Chemistry* **2007,** *28* (7), 1169-1176.
24. Sagara, T.; Ortony, J.; Ganz, E., New isoreticular metal-organic framework materials for high hydrogen storage capacity. *Journal of Chemical Physics* **2005,** *123* (21), 214707.
25. Sagara, T.; Klassen, J.; Ortony, J.; Ganz, E., Binding energies of hydrogen molecules to isoreticular metal-organic framework materials. *Journal of Chemical Physics* **2005,** *123* (1), 014701.
26. Yang, Q.; Zhong, C., Molecular simulation of adsorption and diffusion of hydrogen in metal-organic frameworks. *Journal of Physical Chemistry B* **2005,** *109* (24), 11862-11864.
27. Yang, Q.; Zhong, C., Molecular simulation of carbon dioxide/methane/hydrogen mixture adsorption in metal− organic frameworks. *The Journal of Physical Chemistry B* **2006,** *110* (36), 17776-17783.

28. Mayo, S. L.; Olafson, B. D.; Goddard, W. A., DREIDING: a generic force field for molecular simulations. *The Journal of Physical Chemistry* **1990,** *94* (26), 8897-8909.
29. Rappe, A. K.; Casewit, C. J.; Colwell, K. S.; Goddard, W. A.; Skiff, W. M., UFF, a full periodic table force field for molecular mechanics and molecular dynamics simulations. *J. Am. Chem. Soc.* **1992,** *114*, 10024.
30. Bobbitt, N. S.; Snurr, R. Q., Molecular modelling and machine learning for high-throughput screening of metal-organic frameworks for hydrogen storage. *Molecular Simulation* **2019**, 1-13.
31. McDaniel, J. G.; Li, S.; Tylianakis, E.; Snurr, R. Q.; Schmidt, J. R., Evaluation of force field performance for high-throughput screening of gas uptake in metal-organic frameworks. *J Phys Chem C* **2015,** *119* (6), 3143-3152.
32. Allen, M. P.; Tildesley, D. J., *Computer simulation of liquids*. Oxford university press: 2017.
33. Hamad, S.; Balestra, S. R.; Bueno-Perez, R.; Calero, S.; Ruiz-Salvador, A. R., Atomic charges for modeling metal–organic frameworks: Why and how. *J Solid State Chem* **2015,** *223*, 144-151.
34. Norrby, P.-O.; Brandt, P., Deriving force field parameters for coordination complexes. *Coordination Chemistry Reviews* **2001,** *212* (1), 79-109.
35. Allinger, N., Calculation of molecular structure and energy by force-field methods. In *Advances in physical organic chemistry*, Elsevier: 1976; Vol. 13, pp 1-82.
36. Andrews, D. H., The relation between the Raman spectra and the structure of organic molecules. *Physical Review* **1930,** *36* (3), 544.
37. Allinger, N. L., Conformational analysis. 130. MM2. A hydrocarbon force field utilizing V1 and V2 torsional terms. *Journal of the American Chemical Society* **1977,** *99* (25), 8127-8134.
38. Nevins, N.; Chen, K.; Allinger, N. L., Molecular mechanics (MM4) calculations on alkenes. *Journal of Computational Chemistry* **1996,** *17* (5-6), 669-694.
39. Allinger, N. L.; Zhou, X.; Bergsma, J., Molecular mechanics parameters. *Journal of Molecular Structure: THEOCHEM* **1994,** *312* (1), 69-83.
40. Weiner, P. K.; Kollman, P. A., AMBER: Assisted model building with energy refinement. A general program for modeling molecules and their interactions. *Journal of Computational Chemistry* **1981,** *2* (3), 287-303.
41. Damm, W.; Frontera, A.; Tirado-Rives, J.; Jorgensen, W., The OPLS Potential Functions for Proteins. Energy Minimization for Crystals of Cyclic Peptides and Crambin. *J. Am. Chem. Soc* **1988,** *110*, 1657-1666.
42. Jorgensen, W. L.; Maxwell, D. S.; Tirado-Rives, J., Development and testing of the OPLS all-atom force field on conformational energetics and properties of organic liquids. *Journal of the American Chemical Society* **1996,** *118* (45), 11225-11236.
43. Williams, D. E., Nonbonded potential parameters derived from crystalline aromatic hydrocarbons. *The Journal of Chemical Physics* **1966,** *45* (10), 3770-3778.

44. Williams, D. E., Nonbonded potential parameters derived from crystalline hydrocarbons. *The Journal of Chemical Physics* **1967,** *47* (11), 4680-4684.
45. Addicoat, M. A.; Vankova, N.; Akter, I. F.; Heine, T., Extension of the universal force field to metal–organic frameworks. *J Chem Theory Comput* **2014,** *10* (2), 880-891.
46. Halgren, T. A., The representation of van der Waals (vdW) interactions in molecular mechanics force fields: potential form, combination rules, and vdW parameters. *Journal of the American Chemical Society* **1992,** *114* (20), 7827-7843.
47. Fang, H.; Demir, H.; Kamakoti, P.; Sholl, D. S., Recent developments in first-principles force fields for molecules in nanoporous materials. *J. Mater. Chem. A* **2014,** *2* (2), 274-291.
48. McDaniel, J. G.; Yu, K.; Schmidt, J., Ab initio, physically motivated force fields for CO2 adsorption in zeolitic imidazolate frameworks. *The Journal of Physical Chemistry C* **2012,** *116* (2), 1892-1903.
49. Li, W.; Grimme, S.; Krieg, H.; Möllmann, J.; Zhang, J., Accurate computation of gas uptake in microporous organic molecular crystals. *The Journal of Physical Chemistry C* **2012,** *116* (16), 8865-8871.
50. Vanduyfhuys, L.; Verstraelen, T.; Vandichel, M.; Waroquier, M.; Van Speybroeck, V., Ab initio parametrized force field for the flexible metal–organic framework mil-53 (al). *J Chem Theory Comput* **2012,** *8* (9), 3217-3231.
51. Mendoza-Cortés, J. L.; Han, S. S.; Goddard III, W. A., High H2 uptake in Li-, Na-, K-metalated covalent organic frameworks and metal organic frameworks at 298 K. *The Journal of Physical Chemistry A* **2012,** *116* (6), 1621-1631.
52. Han, S. S.; Choi, S.-H.; Goddard III, W. A., Improved H2 storage in zeolitic imidazolate frameworks using Li+, Na+, and K+ dopants, with an emphasis on delivery H2 uptake. *The Journal of Physical Chemistry C* **2011,** *115* (8), 3507-3512.
53. Tafipolsky, M.; Schmid, R., Systematic first principles parameterization of force fields for metal− organic frameworks using a genetic algorithm approach. *The Journal of Physical Chemistry B* **2009,** *113* (5), 1341-1352.
54. Fu, J.; Sun, H., An ab initio force field for predicting hydrogen storage in IRMOF materials. *The Journal of Physical Chemistry C* **2009,** *113* (52), 21815-21824.
55. Mendoza-Cortés, J. L.; Han, S. S.; Furukawa, H.; Yaghi, O. M.; Goddard III, W. A., Adsorption mechanism and uptake of methane in covalent organic frameworks: theory and experiment. *The Journal of Physical Chemistry A* **2010,** *114* (40), 10824-10833.
56. Chen, L.; Morrison, C. A.; Düren, T., Improving predictions of gas adsorption in metal–organic frameworks with coordinatively unsaturated metal sites: model potentials, ab initio parameterization, and GCMC simulations. *The Journal of Physical Chemistry C* **2012,** *116* (35), 18899-18909.
57. Han, S. S.; Choi, S.-H.; Goddard III, W. A., Zeolitic imidazolate frameworks as H2 adsorbents: Ab initio based grand canonical monte carlo simulation. *The Journal of Physical Chemistry C* **2010,** *114* (27), 12039-12047.

58. Dzubak, A. L.; Lin, L.-C.; Kim, J.; Swisher, J. A.; Poloni, R.; Maximoff, S. N.; Smit, B.; Gagliardi, L., Ab initio carbon capture in open-site metal–organic frameworks. *Nature chemistry* **2012,** *4* (10), 810.
59. Chen, L.; Grajciar, L.; Nachtigall, P.; Düren, T., Accurate prediction of methane adsorption in a metal–organic framework with unsaturated metal sites by direct implementation of an ab initio derived potential energy surface in GCMC simulation. *The Journal of Physical Chemistry C* **2011,** *115* (46), 23074-23080.
60. Yu, D.; Ghosh, P.; Snurr, R. Q., Hierarchical modeling of ammonia adsorption in functionalized metal–organic frameworks. *Dalton T* **2012,** *41* (14), 3962-3973.
61. Zhang, K.; Zhang, L.; Jiang, J., Adsorption of C1–C4 alcohols in zeolitic imidazolate framework-8: Effects of force fields, atomic charges, and framework flexibility. *The Journal of Physical Chemistry C* **2013,** *117* (48), 25628-25635.
62. Fischer, M.; Kuchta, B.; Firlej, L.; Hoffmann, F.; Fröba, M., Accurate prediction of hydrogen adsorption in metal− organic frameworks with unsaturated metal sites via a combined density-functional theory and molecular mechanics approach. *The Journal of Physical Chemistry C* **2010,** *114* (44), 19116-19126.
63. Haldoupis, E.; Borycz, J.; Shi, H.; Vogiatzis, K. D.; Bai, P.; Queen, W. L.; Gagliardi, L.; Siepmann, J. I., Ab initio derived force fields for predicting CO2 adsorption and accessibility of metal sites in the metal–organic frameworks M-MOF-74 (M= Mn, Co, Ni, Cu). *The Journal of Physical Chemistry C* **2015,** *119* (28), 16058-16071.
64. Zang, J.; Nair, S.; Sholl, D. S., Prediction of water adsorption in copper-based metal–organic frameworks using force fields derived from dispersion-corrected DFT calculations. *The Journal of Physical Chemistry C* **2013,** *117* (15), 7519-7525.
65. Fischer, M.; Gomes, J. R.; Fröba, M.; Jorge, M., Modeling adsorption in metal–organic frameworks with open metal sites: propane/propylene separations. *Langmuir* **2012,** *28* (22), 8537-8549.
66. Yang, Q.; Zhong, C., Understanding hydrogen adsorption in metal− organic frameworks with open metal sites: a computational study. *The Journal of Physical Chemistry B* **2006,** *110* (2), 655-658.
67. Salles, F.; Ghoufi, A.; Maurin, G.; Bell, R. G.; Mellot-Draznieks, C.; Férey, G., Molecular Dynamics Simulations of Breathing MOFs: Structural Transformations of MIL-53 (Cr) upon Thermal Activation and CO2 Adsorption. *Angewandte Chemie International Edition* **2008,** *47* (44), 8487-8491.
68. Tafipolsky, M.; Amirjalayer, S.; Schmid, R., First-principles-derived force field for copper paddle-wheel-based metal− organic frameworks. *The Journal of Physical Chemistry C* **2010,** *114* (34), 14402-14409.
69. Hu, Z.; Zhang, L.; Jiang, J., Development of a force field for zeolitic imidazolate framework-8 with structural flexibility. *The Journal of chemical physics* **2012,** *136* (24), 244703.
70. Lin, H.; Truhlar, D. G., QM/MM: what have we learned, where are we, and where do we go from here? *Theor Chem Acc* **2007,** *117* (2), 185.

71. Zheng, C.; Liu, D.; Yang, Q.; Zhong, C.; Mi, J., Computational study on the influences of framework charges on CO2 uptake in metal− organic frameworks. *Industrial & Engineering Chemistry Research* **2009,** *48* (23), 10479-10484.
72. Yazaydın, A. O. z. r.; Snurr, R. Q.; Park, T.-H.; Koh, K.; Liu, J.; LeVan, M. D.; Benin, A. I.; Jakubczak, P.; Lanuza, M.; Galloway, D. B., Screening of metal− organic frameworks for carbon dioxide capture from flue gas using a combined experimental and modeling approach. *Journal of the American Chemical Society* **2009,** *131* (51), 18198-18199.
73. Babarao, R.; Hu, Z.; Jiang, J.; Chempath, S.; Sandler, S. I., Storage and separation of CO2 and CH4 in silicalite, C168 schwarzite, and IRMOF-1: a comparative study from Monte Carlo simulation. *Langmuir* **2007,** *23* (2), 659-666.
74. Babarao, R.; Jiang, J., Unprecedentedly high selective adsorption of gas mixtures in rho zeolite-like metal− organic framework: a molecular simulation study. *Journal of the American Chemical Society* **2009,** *131* (32), 11417-11425.
75. Colón, Y. J.; Fairen-Jimenez, D.; Wilmer, C. E.; Snurr, R. Q., High-throughput screening of porous crystalline materials for hydrogen storage capacity near room temperature. *The Journal of Physical Chemistry C* **2014,** *118* (10), 5383-5389.
76. Wilmer, C. E.; Leaf, M.; Lee, C. Y.; Farha, O. K.; Hauser, B. G.; Hupp, J. T.; Snurr, R. Q., Large-scale screening of hypothetical metal–organic frameworks. *Nature Chemistry* **2012,** *4* (2), 83.
77. Qiao, Z.; Zhang, K.; Jiang, J., In silico screening of 4764 computation-ready, experimental metal–organic frameworks for CO 2 separation. *Journal of Materials Chemistry A* **2016,** *4* (6), 2105-2114.
78. Watanabe, T.; Sholl, D. S., Accelerating applications of metal–organic frameworks for gas adsorption and separation by computational screening of materials. *Langmuir* **2012,** *28* (40), 14114-14128.
79. Avci, G.; Velioglu, S.; Keskin, S., High-throughput screening of MOF adsorbents and membranes for H2 purification and CO2 capture. *Acs Appl Mater Inter* **2018,** *10* (39), 33693-33706.
80. Altintas, C.; Avci, G.; Daglar, H.; Gulcay, E.; Erucar, I.; Keskin, S., Computer simulations of 4240 MOF membranes for H 2/CH 4 separations: insights into structure–performance relations. *Journal of Materials Chemistry A* **2018,** *6* (14), 5836-5847.
81. Wu, D.; Wang, C.; Liu, B.; Liu, D.; Yang, Q.; Zhong, C., Large-scale computational screening of metal-organic frameworks for CH4/H2 separation. *AIChE Journal* **2012,** *58* (7), 2078-2084.
82. Wu, D.; Yang, Q.; Zhong, C.; Liu, D.; Huang, H.; Zhang, W.; Maurin, G., Revealing the structure–property relationships of metal–organic frameworks for CO_2 capture from flue gas. *Langmuir* **2012,** *28* (33), 12094-12099.
83. Yang, Q.; Zhong, C.; Chen, J.-F., Computational study of CO2 storage in metal− organic frameworks. *The Journal of Physical Chemistry C* **2008,** *112* (5), 1562-1569.

84. Noguchi, D.; Tanaka, H.; Kondo, A.; Kajiro, H.; Noguchi, H.; Ohba, T.; Kanoh, H.; Kaneko, K., Quantum sieving effect of three-dimensional Cu-based organic framework for H2 and D2. *Journal of the American Chemical Society* **2008,** *130* (20), 6367-6372.
85. Wongsinlatam, W.; Remsungnen, T., Molecular dynamics simulations of CO2 molecules in ZIF-11 using refined AMBER force field. *Journal of Chemistry* **2013,** *2013*.
86. Pérez-Pellitero, J.; Amrouche, H.; Siperstein, F. R.; Pirngruber, G.; Nieto-Draghi, C.; Chaplais, G.; Simon-Masseron, A.; Bazer-Bachi, D.; Peralta, D.; Bats, N., Adsorption of CO_2, CH_4, and N_2 on zeolitic imidazolate frameworks: experiments and simulations. *Chemistry–A European Journal* **2010,** *16* (5), 1560-1571.
87. Keskin, S., Gas adsorption and diffusion in a highly CO2 selective metal–organic framework: molecular simulations. *Molecular Simulation* **2013,** *39* (1), 14-24.
88. Rankin, R. B.; Liu, J.; Kulkarni, A. D.; Johnson, J. K., Adsorption and diffusion of light gases in ZIF-68 and ZIF-70: a simulation study. *The Journal of Physical Chemistry C* **2009,** *113* (39), 16906-16914.
89. Fischer, M.; Hoffmann, F.; Fröba, M., Preferred hydrogen adsorption sites in various MOFs—a comparative computational study. *ChemPhysChem* **2009,** *10* (15), 2647-2657.
90. Gee, J. A.; Chung, J.; Nair, S.; Sholl, D. S., Adsorption and diffusion of small alcohols in zeolitic imidazolate frameworks ZIF-8 and ZIF-90. *The Journal of Physical Chemistry C* **2013,** *117* (6), 3169-3176.
91. Boyd, P. G.; Moosavi, S. M.; Witman, M.; Smit, B., Force-field prediction of materials properties in metal-organic frameworks. *The journal of physical chemistry letters* **2017,** *8* (2), 357-363.
92. Sumer, Z.; Keskin, S., Ranking of MOF Adsorbents for CO2 Separations: A Molecular Simulation Study. *Industrial & Engineering Chemistry Research* **2016,** *DOI:10.1021/acs.iecr.6b02585*.
93. Chung, Y. G.; Camp, J.; Haranczyk, M.; Sikora, B. J.; Bury, W.; Krungleviciute, V.; Yildirim, T.; Farha, O. K.; Sholl, D. S.; Snurr, R. Q., Computation-ready, experimental metal–organic frameworks: A tool to enable high-throughput screening of nanoporous crystals. *Chem Mater* **2014,** *26* (21), 6185-6192.
94. Sezginel, K. B.; Uzun, A.; Keskin, S., Multivariable linear models of structural parameters to predict methane uptake in metal–organic frameworks. *Chem Eng Sci* **2015,** *124*, 125-134.
95. Allen, F. H., The Cambridge Structural Database: a quarter of a million crystal structures and rising. *Acta Crystallographica Section B: Structural Science* **2002,** *58* (3), 380-388.
96. Willems, T. F.; Rycroft, C. H.; Kazi, M.; Meza, J. C.; Haranczyk, M., Algorithms and tools for high-throughput geometry-based analysis of crystalline porous materials. *Micropor Mesopor Mat* **2012,** *149* (1), 134-141.

97. Sarkisov, L.; Harrison, A., Computational structure characterisation tools in application to ordered and disordered porous materials. *Molecular Simulation* **2011,** *37* (15), 1248-1257.
98. Smit, B., Phase diagrams of Lennard-Jones fluids. *The Journal of Chemical Physics* **1992,** *96* (11), 8639-8640.
99. Potoff, J. J.; Siepmann, J. I., Vapor–liquid equilibria of mixtures containing alkanes, carbon dioxide, and nitrogen. *AIChE Journal* **2001,** *47* (7), 1676-1682.
100. Makrodimitris, K.; Papadopoulos, G. K.; Theodorou, D. N., Prediction of permeation properties of CO_2 and N_2 through silicalite via molecular simulations. *The Journal of Physical Chemistry B* **2001,** *105* (4), 777-788.
101. Buch, V., Path integral simulations of mixed para-D2 and ortho-D2 clusters: The orientational effects. *The Journal of Chemical Physics* **1994,** *100* (10), 7610-7629.
102. Martin, M. G.; Siepmann, J. I., Transferable potentials for phase equilibria. 1. United-atom description of n-alkanes. *The Journal of Physical Chemistry B* **1998,** *102* (14), 2569-2577.
103. Wilmer, C. E.; Kim, K. C.; Snurr, R. Q., An extended charge equilibration method. *The journal of physical chemistry letters* **2012,** *3* (17), 2506-2511.
104. Wei, L.; Zizhen, R.; Chung, Y.; Li, S., The Role of Partial Atomic Charge Assignment Methods on the Computational Screening of Metal-Organic Frameworks for CO2 Capture under Humid Conditions. *Chemistry Select* **2017,** *2* (29), 9458–9465.
105. Greathouse, J. A.; Allendorf, M. D., Force field validation for molecular dynamics simulations of IRMOF-1 and other isoreticular zinc carboxylate coordination polymers. *The Journal of Physical Chemistry C* **2008,** *112* (15), 5795-5802.
106. Haldoupis, E.; Watanabe, T.; Nair, S.; Sholl, D. S., Quantifying Large Effects of Framework Flexibility on Diffusion in MOFs: CH_4 and CO_2 in ZIF-8. *ChemPhysChem* **2012,** *13* (15), 3449-3452.
107. Bae, Y. S.; Snurr, R. Q., Development and evaluation of porous materials for carbon dioxide separation and capture. *Angewandte Chemie International Edition* **2011,** *50* (49), 11586-11596.
108. Rege, S. U.; Yang, R. T., A simple parameter for selecting an adsorbent for gas separation by pressure swing adsorption. *Separation science and technology* **2001,** *36* (15), 3355-3365.
109. Dubbeldam, D.; Calero, S.; Ellis, D. E.; Snurr, R. Q., RASPA: molecular simulation software for adsorption and diffusion in flexible nanoporous materials. *Molecular Simulation* **2016,** *42* (2), 81-101.
110. Kristóf, T.; Liszi, J., Effective intermolecular potential for fluid hydrogen sulfide. *The Journal of Physical Chemistry B* **1997,** *101* (28), 5480-5483.
111. Hamon, L.; Serre, C.; Devic, T.; Loiseau, T.; Millange, F.; Férey, G.; Weireld, G. D., Comparative study of hydrogen sulfide adsorption in the MIL-53 (Al, Cr, Fe), MIL-47 (V), MIL-100 (Cr), and MIL-101 (Cr) metal− organic frameworks at room temperature. *Journal of the American Chemical Society* **2009,** *131* (25), 8775-8777.

112. Peng, X.; Cao, D., Computational screening of porous carbons, zeolites, and metal organic frameworks for desulfurization and decarburization of biogas, natural gas, and flue gas. *AIChE Journal* **2013,** *59* (8), 2928-2942.
113. Wang, S.; Wu, D.; Huang, H.; Yang, Q.; Tong, M.; Liu, D.; Zhong, C., Computational exploration of H2S/CH4 mixture separation using acid-functionalized UiO-66 (Zr) membrane and composites. *Chinese Journal of Chemical Engineering* **2015,** *23* (8), 1291-1299.
114. Sokhanvaran, V.; Gomar, M.; Yeganegi, S., H2S separation from biogas by adsorption on functionalized MIL-47-X (X=− OH and− OCH3): A simulation study. *Appl Surf Sci* **2019,** *479*, 1006-1013.
115. Vaesen, S.; Guillerm, V.; Yang, Q.; Wiersum, A. D.; Marszalek, B.; Gil, B.; Vimont, A.; Daturi, M.; Devic, T.; Llewellyn, P. L., A robust amino-functionalized titanium (IV) based MOF for improved separation of acid gases. *Chem Commun* **2013,** *49* (86), 10082-10084.
116. Shah, M. S.; Tsapatsis, M.; Siepmann, J. I., Monte Carlo simulations probing the adsorptive separation of hydrogen sulfide/methane mixtures using all-silica zeolites. *Langmuir* **2015,** *31* (44), 12268-12278.
117. Xu, J.; Sang, P.; Zhao, L.; Xing, W.; Yan, Z. In *Adsorption and Separation of H2S in HKUST-1 Metal Organic Frameworks: A Monte Carlo Simulation Study*, 5th International Conference on Information Engineering for Mechanics and Materials, Atlantis Press: 2015.
118. Al-Jadir, T. M.; Siperstein, F. R., The influence of the pore size in Metal− Organic Frameworks in adsorption and separation of hydrogen sulphide: A molecular simulation study. *Micropor Mesopor Mat* **2018,** *271*, 160-168.
119. Bobbitt, N. S.; Mendonca, M. L.; Howarth, A. J.; Islamoglu, T.; Hupp, J. T.; Farha, O. K.; Snurr, R. Q., Metal–organic frameworks for the removal of toxic industrial chemicals and chemical warfare agents. *Chemical Society Reviews* **2017,** *46* (11), 3357-3385.
120. Li, Z.; Xiao, Y.; Xue, W.; Yang, Q.; Zhong, C., Ionic liquid/metal–organic framework composites for H2S removal from natural gas: A computational exploration. *The Journal of Physical Chemistry C* **2015,** *119* (7), 3674-3683.
121. Li, Z.; Liao, F.; Jiang, F.; Liu, B.; Ban, S.; Chen, G.; Sun, C.; Xiao, P.; Sun, Y., Capture of H2S and SO2 from trace sulfur containing gas mixture by functionalized UiO-66 (Zr) materials: A molecular simulation study. *Fluid Phase Equilibr* **2016,** *427*, 259-267.
122. Xu, H.; Tong, M.-M.; Wu, D.; Xiao, G.; Yang, Q.-Y.; Liu, D.-H.; Zhong, C.-L., Computational study of metal-organic frameworks for removing H2S from natural gas. *Acta Physico-Chimica Sinica* **2015,** *31* (1), 41-50.

APPENDICES

Appendix A. Structural Properties of MOFs

REFCODE	LCD (Å)	PLD (Å)	Surface Area (m^2/g)	Pore Volume (cm^3/g)	REFCODE	LCD (Å)	PLD (Å)	Surface Area (m^2/g)	Pore Volume (cm^3/g)
ACODED	5.52	3.38	314.49	0.43	KUGZIW	10.79	9.76	1331.61	0.65
ACUFEK	13.16	7.60	3558.03	1.31	LARVIL	7.32	7.08	347.97	0.24
AHORAR	6.63	4.31	1259.53	0.67	LASPOM	3.96	2.97	448.80	0.26
AJIHOQ	8.41	6.67	930.28	0.48	LECQEQ	11.46	10.71	1242.20	0.54
AVEROJ	6.88	6.49	654.75	0.34	LUKLIN	16.96	9.39	3955.12	1.61
BERGAI01	5.10	2.39	796.08	0.28	LUMDIG	7.91	4.95	880.17	0.42
BEYSEF	4.85	3.93	599.19	0.48	LUXDEO	5.05	2.36	1708.95	0.36
BOWSIQ	4.53	2.99	781.23	0.34	MOCKAR	10.86	6.77	2918.74	1.00
BUVWOF02	6.27	4.71	354.90	0.32	MOCKEV	10.91	3.75	2154.65	0.86
DEJROB	4.93	2.89	1090.32	0.39	NEFTOJ	4.65	3.63	1049.96	0.56
DIDBID	8.83	5.23	1133.64	0.59	NIBHOW	22.93	14.89	5202.76	3.03
DIDBOJ	8.82	5.29	1129.16	0.59	NIMPEG01	5.87	5.25	2557.83	0.88
EBAMOL	7.71	3.61	570.73	0.53	NUJCIE	4.30	3.45	176.25	0.28
EBEMOO	4.13	3.10	211.72	0.22	NUTQAV	10.91	4.12	2772.48	0.94
EDUSIF	15.06	7.93	3685.93	1.36	NUTQEZ	11.70	4.31	2392.98	0.81
EDUSUR	14.97	6.61	2675.83	1.06	OCIZIL	4.79	3.72	90.76	0.31
EDUVII	20.32	9.78	4540.87	2.03	OFERUN	11.14	2.79	1617.54	0.64
EDUVOO	20.94	10.64	4847.41	2.31	OHUKIM	14.71	8.30	4642.30	1.88
EHALOP	7.52	7.08	1671.71	0.69	OWITAQ	7.59	5.36	4752.93	1.18
EMIHAK	9.39	5.69	1313.24	0.45	OWITEU	7.56	5.32	4837.06	1.19
EMIHIS	9.39	5.69	1313.24	0.45	OWITIY	7.66	5.80	5105.51	1.30
EMIVAY	4.41	3.66	399.66	0.37	OWITOE	7.52	5.28	4809.83	1.17
EYOPOY	5.88	5.04	715.47	0.45	OWITUK	7.56	5.32	4875.38	1.19
EYOPUE	5.97	5.06	328.74	0.38	OWIVAS	7.56	5.34	4707.92	1.17
EYOQAL	5.85	5.17	369.39	0.37	OWIVEW	6.91	4.45	3152.82	0.86
EZILUV	9.32	3.50	683.87	0.63	PEQHOK	5.24	2.58	970.33	0.31
EZIMAC	9.34	3.50	671.44	0.63	PEVQEO	14.85	7.96	3614.62	1.33
FAYPUS	13.62	4.26	1598.02	0.78	PODKUQ	22.15	8.48	4273.23	1.78
FECXUI	10.11	5.68	1815.60	0.70	PURQOJ	11.31	6.85	2364.67	0.82
FEVFUJ	11.00	10.18	1826.46	0.83	QIFLOI	5.40	3.00	490.00	0.13
FIQCEN	11.12	5.24	1823.14	0.72	QOWQUO	16.36	2.71	2797.39	0.90

REFCODE	LCD (Å)	PLD (Å)	Surface Area (m^2/g)	Pore Volume (cm^3/g)	REFCODE	LCD (Å)	PLD (Å)	Surface Area (m^2/g)	Pore Volume (cm^3/g)
GALBUS	9.07	6.25	1368.15	0.62	RAYKEJ	9.59	7.36	1000.19	0.54
GALHUY	9.78	4.70	2225.98	0.79	RAYKIN	9.48	7.12	968.14	0.53
GITTUZ	10.86	8.04	1169.97	0.60	RAYKUZ	8.95	5.83	936.93	0.52
GITVEL	15.25	13.38	2177.20	0.94	RAYLAG	8.06	5.70	932.94	0.51
GIVDUL	6.31	4.76	704.16	0.32	RAYLEK	8.03	5.63	890.67	0.51
GIWNUV	4.28	1.79	126.70	0.14	RAYLIO	7.61	5.06	953.14	0.49
GUPCOK	7.33	4.70	973.12	0.56	RAYLOU	6.83	5.20	984.01	0.48
GUPDIF	4.02	3.18	308.58	0.36	RAYLUA	6.56	4.80	916.67	0.48
GUSLUC	4.66	3.70	270.70	0.35	SAHYIK	13.33	7.64	3445.98	1.31
HAJKIO	6.67	3.47	801.32	0.39	SOQSAU	9.55	4.98	2420.70	0.81
HAJKOU	6.23	3.27	892.17	0.39	SOQSEY	10.25	4.93	1987.79	0.76
HASSUR	7.03	5.33	1831.69	0.63	VEJYOZ	8.47	5.70	2016.54	0.78
HECQUB	8.60	5.10	2679.72	0.88	VEJZIU	12.35	7.49	2010.53	0.84
HIFVUO	7.50	5.98	2382.16	0.87	VOGTIV	9.85	8.26	1300.53	0.58
IDIWOH	7.68	7.19	1534.78	0.63	WOBHIF	11.58	10.81	1167.10	0.52
IMIXEI	7.09	5.53	2886.52	0.89	XALXUF01	16.56	6.67	2201.90	0.93
JENKIX	9.92	7.49	1105.15	0.56	YOZBIZ01	8.89	6.10	803.24	0.48
KARLAS	7.97	4.30	855.13	0.57	YOZBOF	8.00	4.95	426.36	0.43
KEYFIF	5.40	4.90	214.08	0.25	YUVSUE	5.76	4.59	851.70	0.44
KEYFIF01	5.33	4.84	191.96	0.24	ZELROZ	18.64	12.41	4912.93	2.67
KIPKIF	10.42	10.33	612.78	0.50					

Appendix B. Supplementary Information for Chapter 4

Table B1. Potential parameters of the MOF atoms in UFF and Dreiding

Atom	σ_{UFF}(Å)	ε_{UFF}(K)	$\sigma_{Dreiding}$(Å)	$\varepsilon_{Dreiding}$(K)
Ag	2.80	18.13	2.80	18.13
Al	4.01	254.30	3.91	151.07
Be	2.45	42.80	2.45	42.80
C	3.43	52.87	3.47	47.89
Cd	2.54	114.81	2.54	114.81
Co	2.56	7.05	2.56	7.05
Cu	3.11	2.52	3.11	2.52
Fe	2.59	6.55	2.59	6.55
H	2.57	22.16	2.85	7.65
In	3.98	301.63	4.09	276.96
Mn	2.64	6.55	2.64	6.55
N	3.26	34.75	3.26	38.98
Ni	2.52	7.55	2.52	7.55
O	3.12	30.21	3.03	48.19
V	2.80	8.06	2.80	8.06
Zn	2.46	62.44	4.04	27.70
Zr	2.78	34.75	2.78	34.75

Table B2. The number of common MOFs in top 10 material rankings based on molecular simulations performed using Dreiding and UFF.

Performance evaluation metrics	CO_2/H_2	CO_2/N_2	CO_2/CH_4
S	8	8	9
ΔN (mol/kg)	6	6	8
S_{sp}	8	7	7
R (%)	7	8	8

Table B3. The Spearman's ranking correlation coefficient (SRCC) between Dreiding-based and UFF-based rankings of 100 MOFs.

All MOFs	CO_2/H_2	CO_2/N_2	CO_2/CH_4
S	0.9795	0.9826	0.9774
ΔN (mol/kg)	0.9567	0.9568	0.9521
S_{sp}	0.9774	0.9796	0.9726
R (%)	0.9635	0.9693	0.9699

Table B4. The five MOFs with the highest and lowest FFFs.

MOF	C	H	O	N	Metals	Others	FFF
EMIHAK	144	144	0	32	80 (In)	128 (S)	0.003
OWITIY	148	52	96	0	20 (Mn)	0	0.011
OWITAQ	144	48	96	0	16 (Zn)	0	0.014
OWIVAS	144	48	96	0	16 (Zn)	0	0.014
AVEROJ	12	12	0	18	6 (Cd)	6 (Cl)	0.014
FAYPUS	680	640	128	144	40 (Zn)	0	0.294
NUJCIE	56	80	0	48	8/8 (Cd/Ni)	0	0.333
OFERUN	96	120	0	48	12 (Zn)	0	0.387
LUXDEO	152	184	8	40	8 (Ag)	0	0.418
GUPCOK	480	672	0	192	48 (Cd)	0	0.466

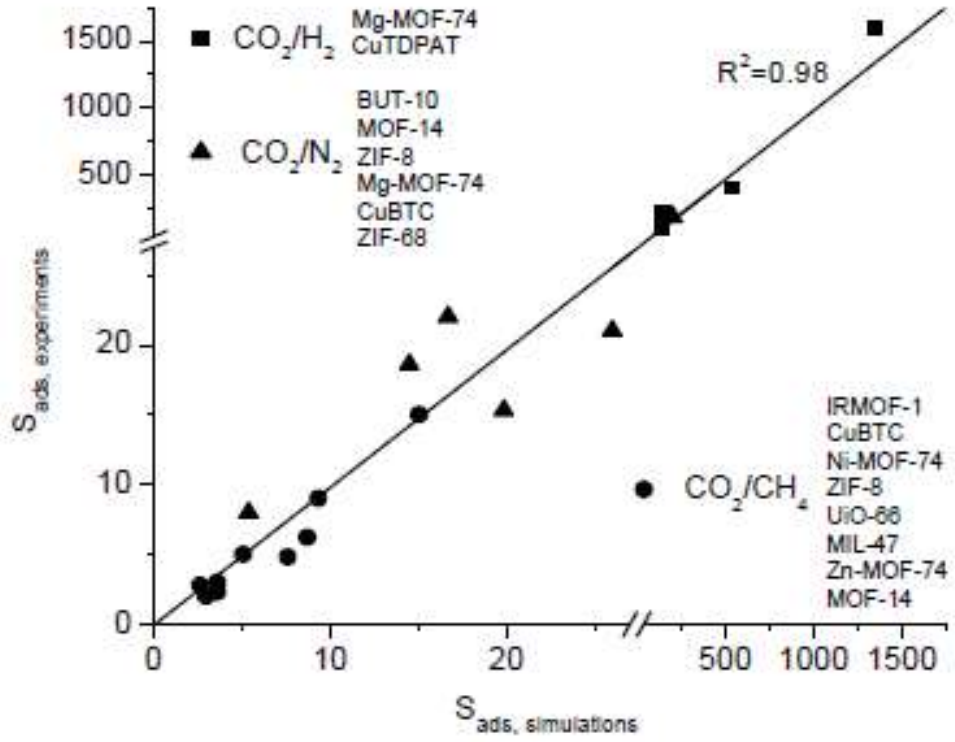

Figure B1. Comparison of simulation results with the experiments for CO_2/H_2, CO_2/N_2 and CO_2/CH_4 selectivities of various MOFs. The details of selectivity measurements can be seen in our previous publication.[92]

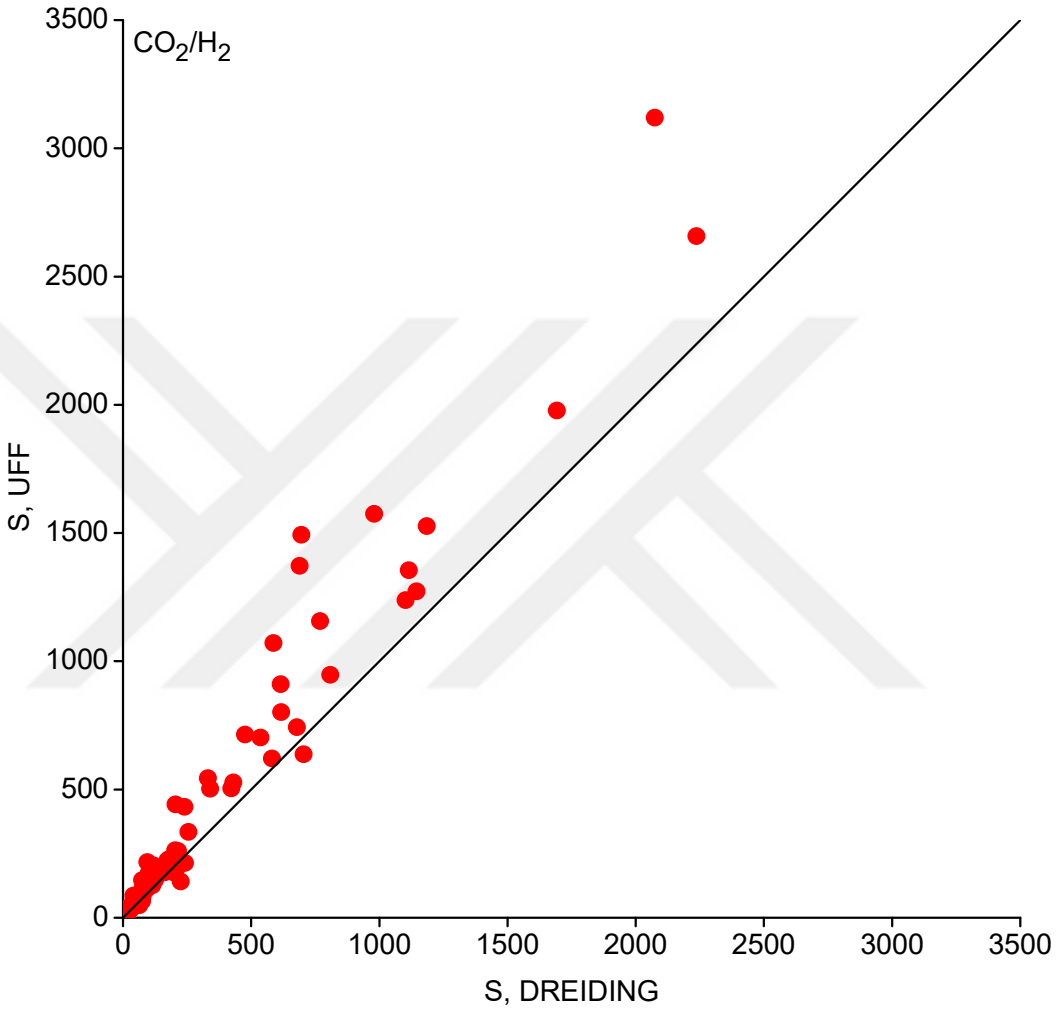

Figure B2. Comparison of CO_2/H_2 selectivities of MOFs calculated with Dreiding and UFF at 1 bar.

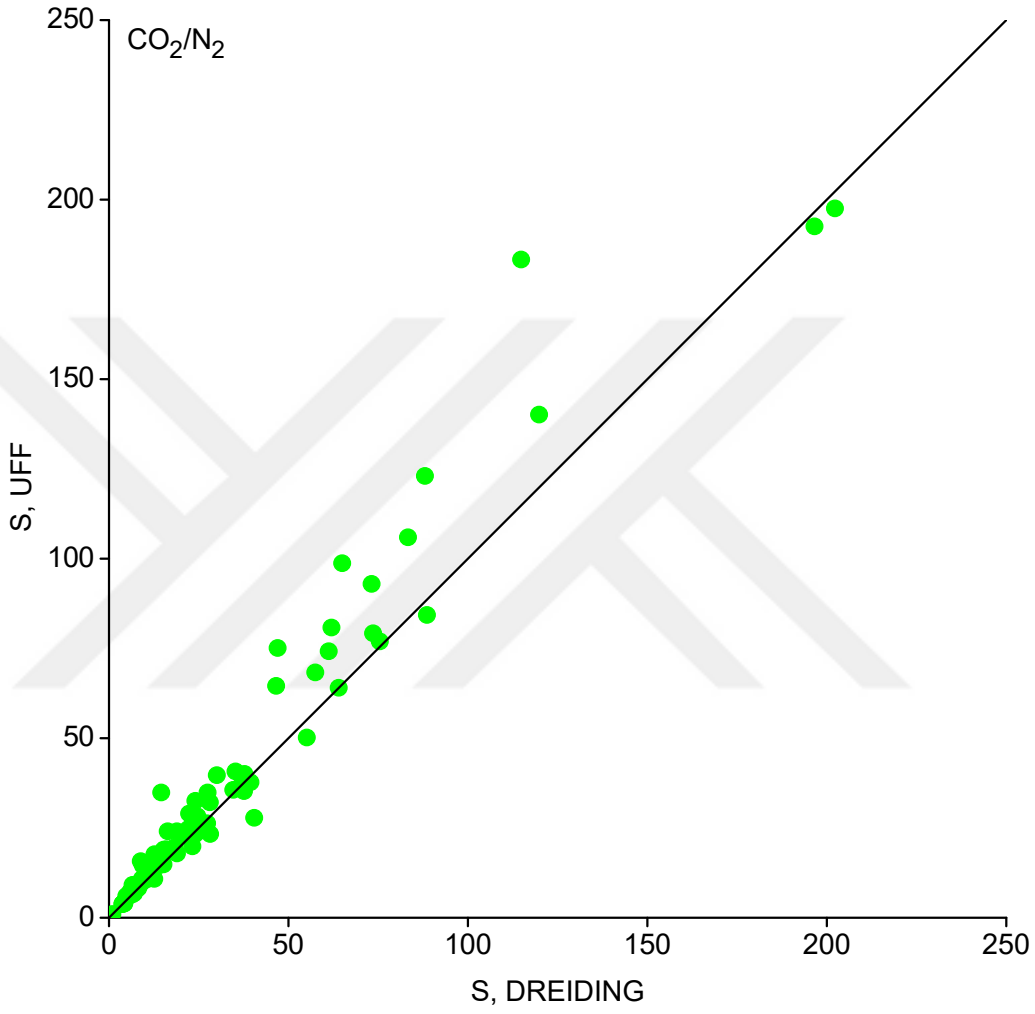

Figure B3. Comparison of CO_2/N_2 selectivities of MOFs calculated with Dreiding and UFF at 1 bar.

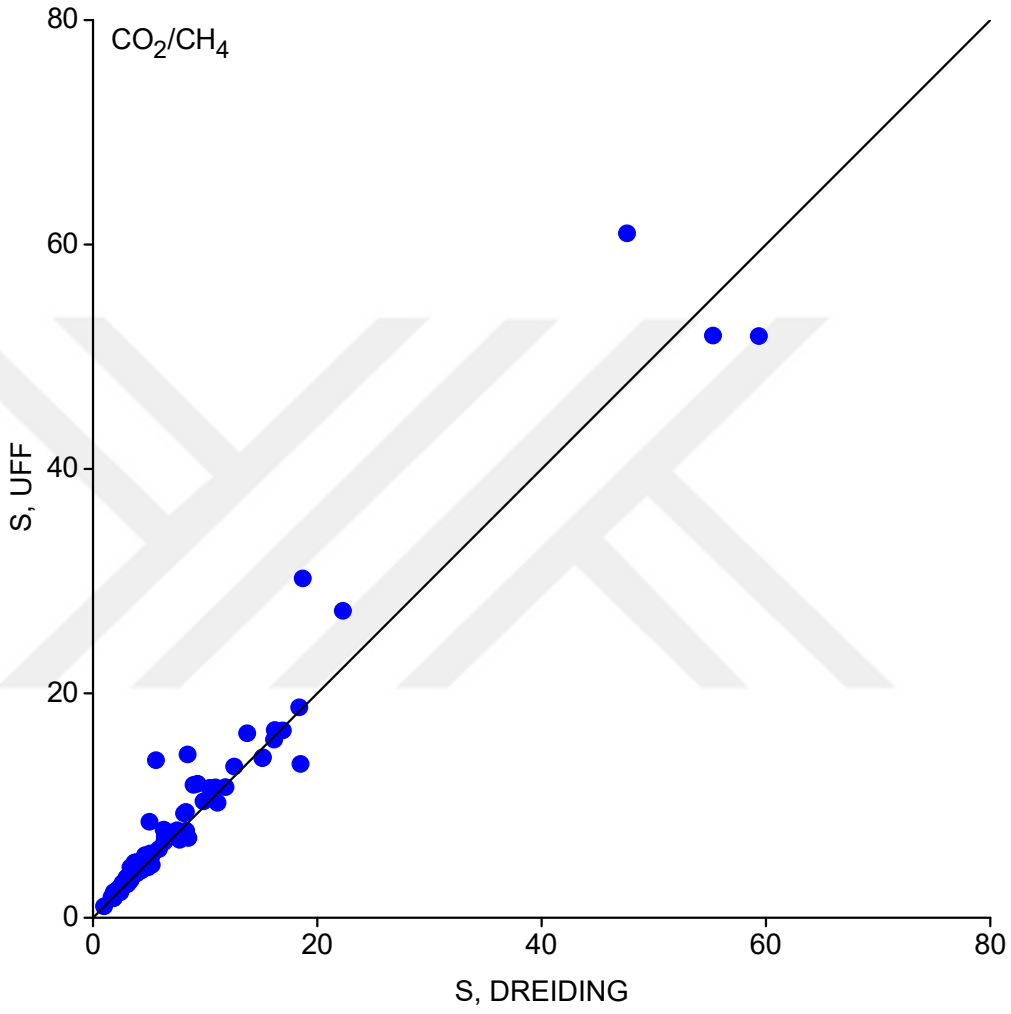

Figure B4. Comparison of CO_2/CH_4 selectivities of MOFs calculated with Dreiding and UFF at 1 bar.

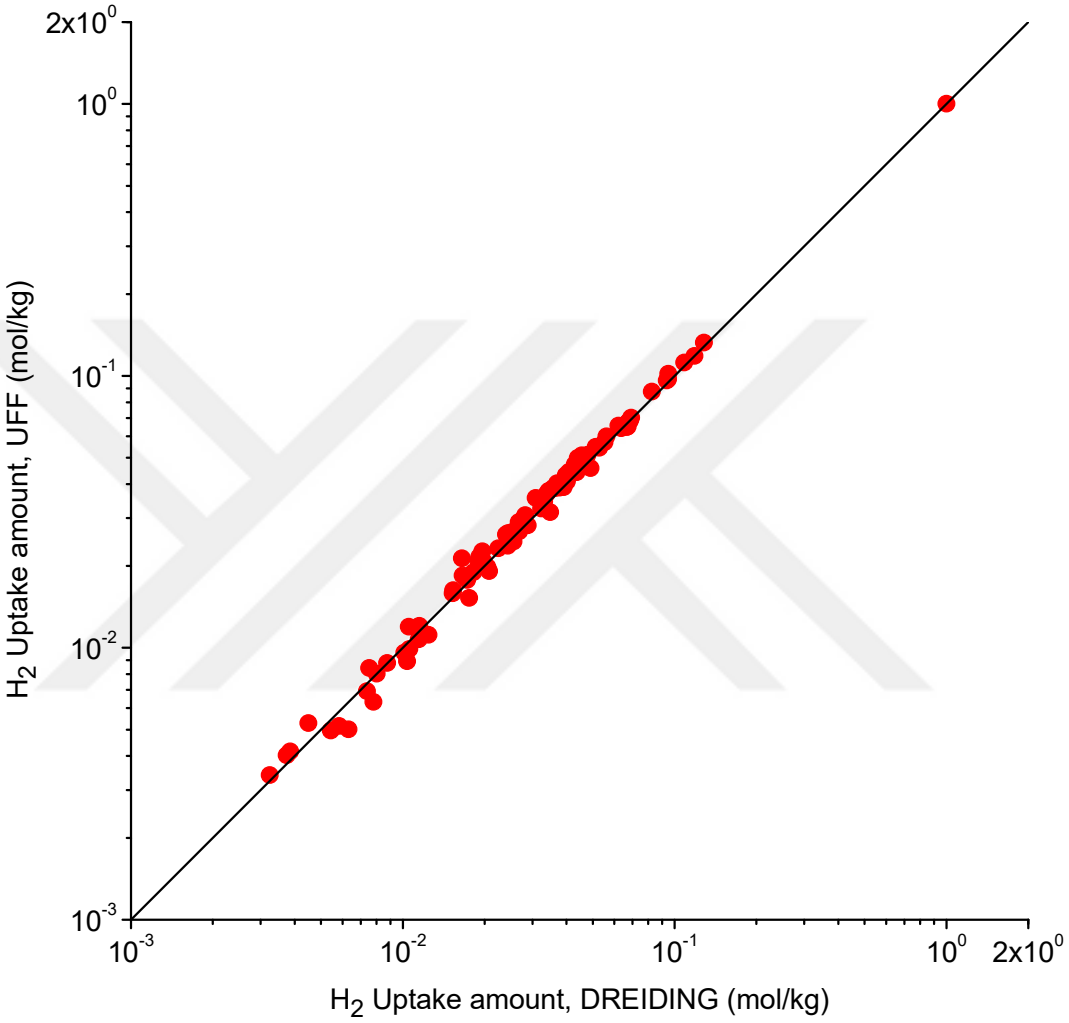

Figure B5. Comparison of H_2 uptakes of MOFs for CO_2/H_2 mixture calculated with Dreiding and UFF at 1 bar.

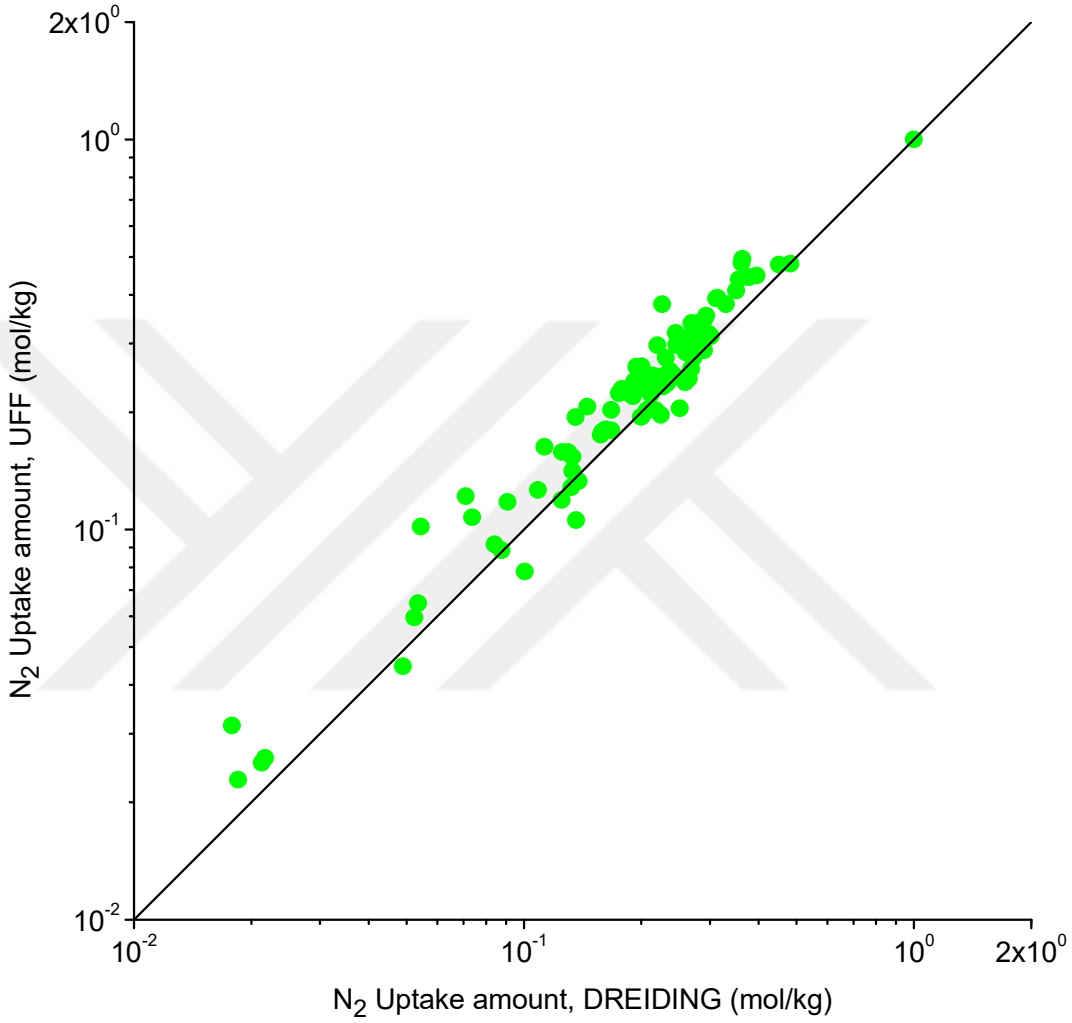

Figure B6. Comparison of N_2 uptakes of MOFs for CO_2/N_2 mixture calculated with Dreiding and UFF at 1 bar.

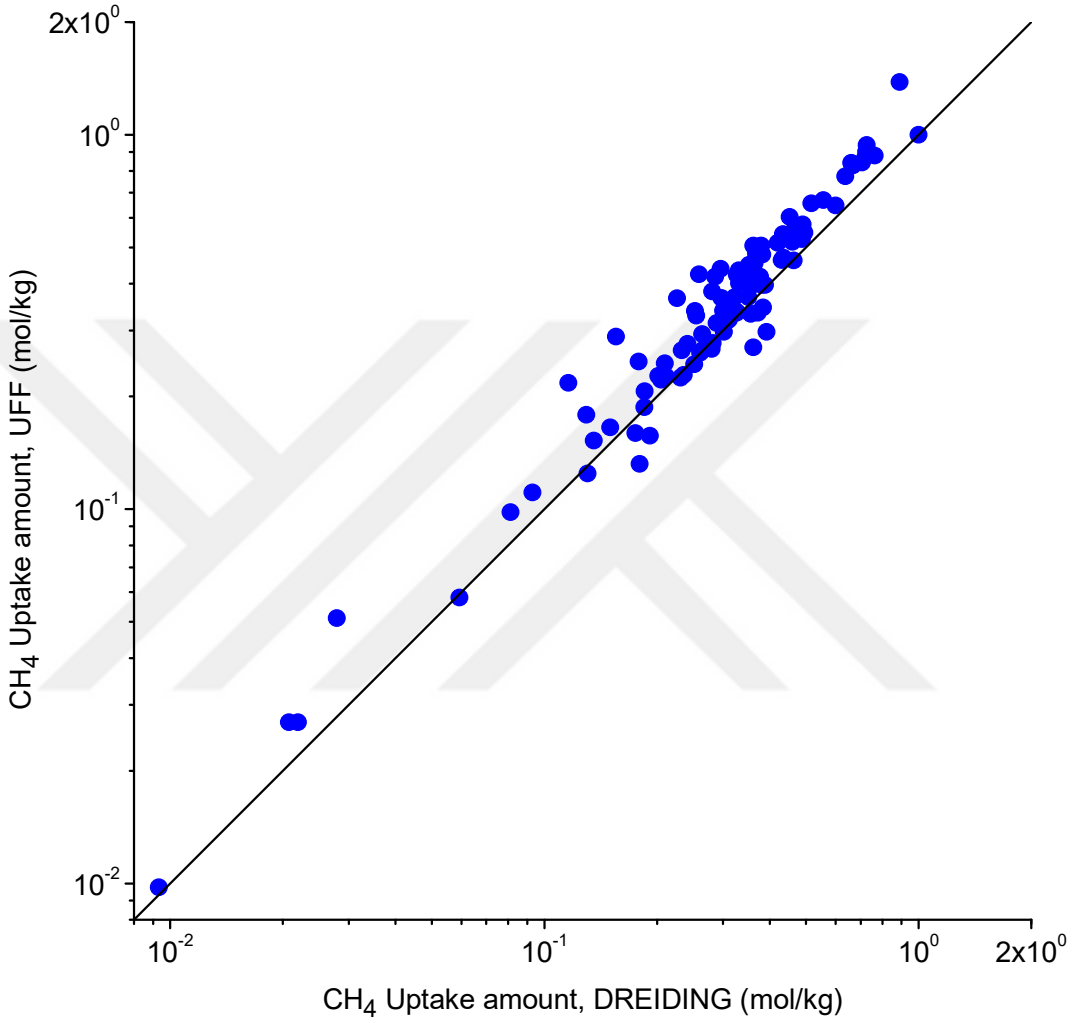

Figure B7. Comparison of CH_4 uptakes of MOFs for CO_2/CH_4 mixture calculated with Dreiding and UFF at 1 bar.

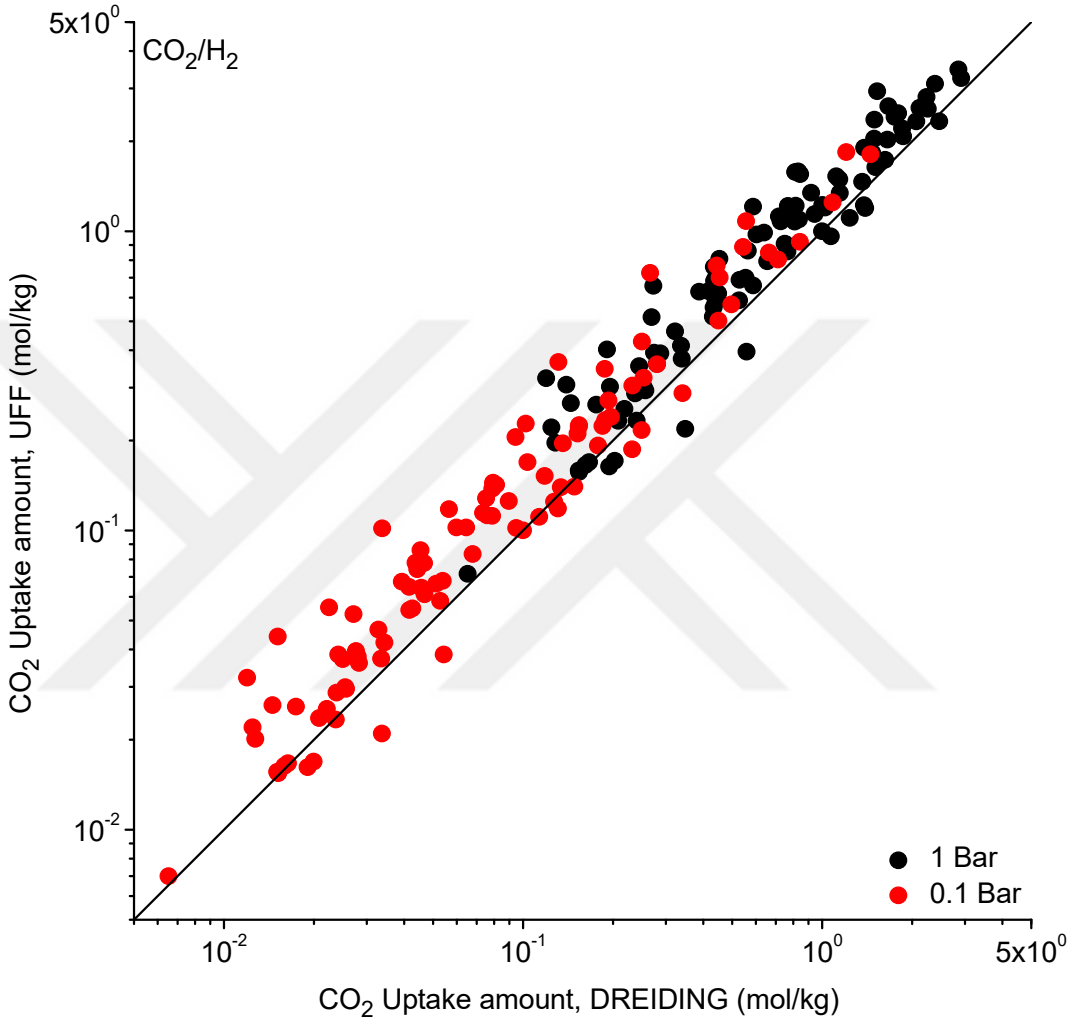

Figure B8. Comparison of CO_2 uptakes of MOFs for CO_2/H_2 mixture calculated with Dreiding and UFF at 0.1 and 1 bar.

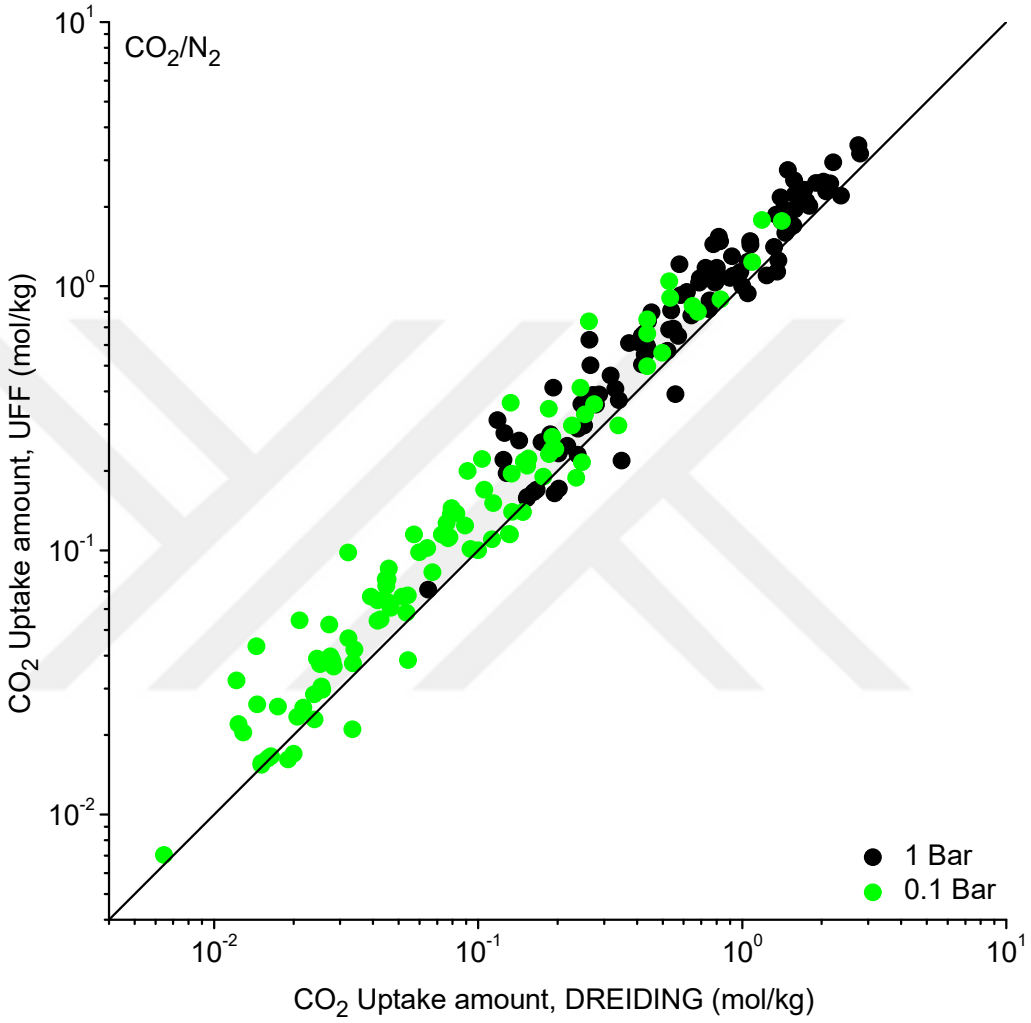

Figure B9. Comparison of CO_2 uptakes of MOFs for CO_2/N_2 mixture calculated with Dreiding and UFF at 0.1 and 1 bar.

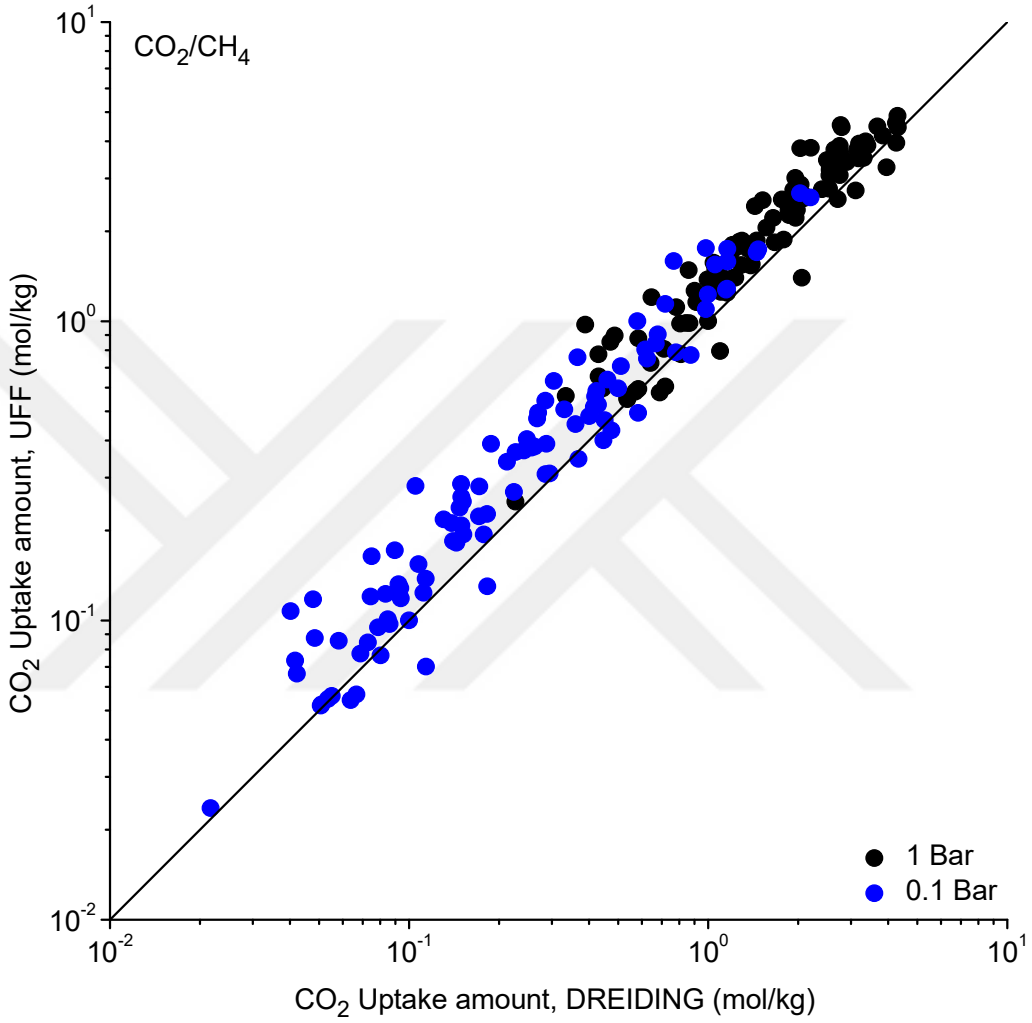

Figure B10. Comparison of CO_2 uptakes of MOFs for CO_2/CH_4 mixture calculated with Dreiding and UFF at 0.1 and 1 bar.

VITA

Derya Dokur was born in Istanbul, Turkey on January 24, 1989. She graduated with a double major from the Departments of Environmental Engineering and Chemical Engineering of Istanbul Technical University in 2015 and 2016, respectively. She successfully got her M.Sc. degree from the Department of Chemical and Biological Engineering of Koç University. She is currently working at Turkish Petroleum Refineries Corporation as the Operations Supervisor at the Production Department.

Publications:

- Dokur, D. and Keskin, S. (2018) "Effects of Force Field Selection on the Computational Ranking of MOFs for CO_2 Separations" Ind. Eng. Chem. Res. 2018, 57, 2298−2309.